HHS Public Access

Author manuscript

Cell Microbiol. Author manuscript; available in PMC 2016 June 03.

Published in final edited form as:

Cell Microbiol. 2016 February ; 18(2): 260–281. doi:10.1111/cmi.12500.

Anaplasma phagocytophilum Rab10-dependent parasitism of the *trans*-Golgi network is critical for completion of the infection cycle

*For correspondence. ; Email: jacarlyon@vcu.edu; Tel. (+804) 628 3382; Fax (+804) 828 9946

†Current Address: Department of Microbiology and Immunology, Northwestern University Feinberg School of Medicine, Chicago, IL, USA.

Author contributions

H. K. T. and J. A. C. designed the experiments, analysed results and wrote the paper. H. K. T., L. V., C. L. C. and N. O. performed the experiments. B. P. G., D. S. W. and C. E. C. performed and analysed data generated by UPLC-ESI-MS/MS.

Supporting information

Additional Supporting Information may be found in the online version of this article at the publisher's web-site:

Fig. S1. The Golgi apparatus is fragmented in *Anaplasma phagocytophilum*-infected host cells with high bacterial burdens. (A) The Golgi apparatus is intact, compact and perinuclear in uninfected host cells. RF/6A cells were screened with antibodies against GM130, GolgB1 or TGN46. (B) The *trans*-Golgi network (TGN) is fragmented in host cells having high *A. phagocytophilum* burdens. RF/6A cells were infected with different loads of *A. phagocytophilum* organisms for 28–32 h and processed for laser scanning confocal microscopy (LSCM). *A. phagocytophilum*-occupied vacuoles (ApVs) were visualized with antibody against the intermediate filament protein, vimentin, which cages ApVs. The TGN and TGN-derived vesicles delivered into the ApV were visualized with TGN46 antibody. (C) The *cis*-Golgi and *medial*-Golgi are fragmented in host cells having high *A. phagocytophilum* burdens. Heavily infected RF/6A cells were screened with antibodies targeting the *cis*-Golgi (GM130 and GolgB1) and *medial*-Golgi (GolgB1). *A. phagocytophilum*-occupied vacuolar membranes and intravacuolar bacteria were visualized with APH0032 antibody. The cells were examined by confocal microscopy. Host cell nuclei and bacterial DNA were stained with 4′,6-diamidino-2-phenylindole (DAPI) (blue). Hatched-line boxes indicate regions that were magnified in the enlargement panels. Data are representative of two experiments with similar results.

Fig. S2. Host cell-free *A. phagocytophilum* reticulate cells (RCs) are Rab10 and TGN46 positive, while host cell-free dense-core morphotypes (DCs) are Rab10 and TGN46 negative. *A. phagocytophilum* RC and DC organisms were isolated from infected HL-60 cells, fixed to glass slides, screened with antibodies against (A) Rab10, (B) TGN46 or (C) P44 and examined by LSCM. Bacterial DNA was stained with DAPI (blue). Results shown are representative of three experiments with similar results.

Fig. S3. HEK-293T cells are appropriate for assessing the effects of Rab10 knockdown on *A. phagocytophilum* infection and Golgi recruitment to the ApV. (A) Green fluorescent protein (GFP)-Rab10 localizes to ApVs in HEK-293T cells. HEK-293T cells were transfected to express GFP-Rab10 for 24 h and subsequently incubated with *A. phagocytophilum*. After 48 h, the cells were processed for LSCM. Bacteria were visualized with antibody against major surface protein P44. Arrow points to an ApV surrounded by a GFP-Rab10 signal. An arrow denotes pronounced GFP-Rab10 signal localized to an ApV. (B) TGN vesicles are delivered into ApVs in HEK-293T cells. *A. phagocytophilum*-infected HEK-293T cells were screened with antibodies against TGN46 and APH0032 and examined by LSCM. (C) The Golgi is intact following Rab10 knockdown in HEK-293T cells. HEK-293T cells were treated with non-targeting or Rab10-targeting small interfering RNA. After 72 h, the cells were fixed and processed for confocal microscopy. The Golgi was visualized with TGN46 antibody. (A–C) Host cell nuclei and bacterial DNA were visualized with DAPI (blue). Data are representative of two experiments with similar results.

Fig. S4. Halo-uridine monophosphate kinase (UMPK) and GFP, Halo and GFP-Rab10 and Halo-tagged *Escherichia coli* UMPK and GFP-Rab10 fail to colocalize when coexpressed in HeLa cells. (A–C) Transfected HeLa cells expressing Halo-UMPK and GFP (A), Halo alone and GFP-Rab10 (B) or Halo-tagged *E. coli* UMPK and GFP-Rab10 (C) were examined using confocal microscopy. Host cell nuclei were stained with DAPI (blue). Data are representative of two experiments with similar results.

Fig. S5. Validation of antibody specific for UMPK amino acids 182–195. (A) Western blot of uninfected or *A. phagocytophilum*-infected RF/6A cell lysates probed with UMPK antibody detects a band having an apparent molecular weight of approximately 26 kDa, which corresponds to the expected size of UMPK, in the infected cell lysate only. Data are representative of two experiments with similar results. (B) UMPK is constitutively expressed throughout infection. RF/6A cells were synchronously infected with *A. phagocytophilum* for 4, 8, 12, 16, 24, 28 or 32 h, after which, the cells were fixed, screened with UMPK antibody, stained with DAPI and examined by confocal microscopy. Results shown are representative of three experiments. Statistically significant (***$P \leq 0.001$; *$P \leq 0.05$) values are indicated.

Movie S1. Endogenous Rab10-positive vesicles colocalize with intravacuolar *A. phagocytophilum* organisms. *A. phagocytophilum* infected RF/6A cells were screened with antibodies against Rab10 (red) and APH0032 (green), stained with DAPI (blue) and visualized by LSCM. Z-stack images obtained for a representative ApV in Fig. 1D were used for three-dimensional rendering.

Movie S2. TGN-derived vesicles colocalize with intravacuolar *A. phagocytophilum* organisms. *A. phagocytophilum*-infected RF/6A cells were screened with antibodies against TGN46 (red) and APH0032 (green), stained with DAPI (blue) and visualized by LSCM. Z-stack images obtained for a representative ApV in Fig. 3B were used for three-dimensional rendering.

Hilary K. Truchan[1,†], **Lauren VieBrock**[1], **Chelsea L. Cockburn**[1], **Nore Ojogun**[1], **Brian P. Griffin**[2], **Dayanjan S. Wijesinghe**[3,4], **Charles E. Chalfant**[4,5,6,7,8], and **Jason A. Carlyon**[1,2,*]

[1]Department of Microbiology and Immunology, Virginia Commonwealth University School of Medicine, Richmond, VA, USA

[2]Molecular Biology and Genetics Program, Virginia Commonwealth University School of Medicine, Richmond, VA, USA

[3]Department of Surgery, Virginia Commonwealth University School of Medicine, Richmond, VA, USA

[4]Department of Biochemistry and Molecular Biology, Virginia Commonwealth University School of Medicine, Richmond, VA, USA

[5]Massey Cancer Center, Virginia Commonwealth University School of Medicine, Richmond, VA, USA

[6]The Victoria Johnson Center, Virginia Commonwealth University School of Medicine, Richmond, VA, USA

[7]Institute for Molecular Medicine, Virginia Commonwealth University School of Medicine, Richmond, VA, USA

[8]Research and Development, Hunter Holmes McGuire Veterans Administration Medical Center, Richmond, VA, USA

Summary

Anaplasma phagocytophilum is an emerging human pathogen and obligate intracellular bacterium. It inhabits a host cell-derived vacuole and cycles between replicative reticulate cell (RC) and infectious dense-cored (DC) morphotypes. Host–pathogen interactions that are critical for RC-to-DC conversion are undefined. We previously reported that *A. phagocytophilum* recruits green fluorescent protein (GFP)-tagged Rab10, a GTPase that directs exocytic traffic from the sphingolipid-rich *trans*-Golgi network (TGN) to its vacuole in a guanine nucleotide-independent manner. Here, we demonstrate that endogenous Rab10-positive TGN vesicles are not only routed to but also delivered into the *A. phagocytophilum*-occupied vacuole (ApV). Consistent with this finding, *A. phagocytophilum* incorporates sphingolipids while intracellular and retains them when naturally released from host cells. TGN vesicle delivery into the ApV is Rab10 dependent, up-regulates expression of the DC-specific marker, APH1235, and is critical for the production of infectious progeny. The *A. phagocytophilum* surface protein, uridine monophosphate kinase, was identified as a guanine nucleotide-independent, Rab10-specific ligand. These data delineate why Rab10 is important for the *A. phagocytophilum* infection cycle and expand the understanding of the benefits that exploiting host cell membrane traffic affords intracellular bacterial pathogens.

Introduction

Anaplasma phagocytophilum is a tick-transmitted, obligatory intracellular bacterium that proliferates in membrane-bound inclusions of granulocytes and bone marrow progenitor cells. *A. phagocytophilum* infection in humans, termed human granulocytic anaplasmosis

(HGA), is an emerging zoonosis in the USA, Europe and Asia (reviewed by Truchan *et al*., 2013). HGA presents as an acute febrile illness characterized by chills, headache, malaise, leucopenia, thrombocytopenia and elevated hepatic aminotransferases. More severe complications may include rhabdomyolysis, haemorrhage, shock, seizures, pneumonitis, increased susceptibility to secondary infections and death (Truchan *et al*., 2013). Promyelocytic HL-60, RF/6A endothelial and human embryonic kidney (HEK-293T) cells are useful *in vitro* models for studying *A. phagocytophilum* infection (Klein *et al*., 1997; Munderloh *et al*., 2004; Beyer *et al*., 2014). The bacterium undergoes a biphasic developmental cycle in which an infectious dense-cored (DC) organism invades to reside within a host cell-derived vacuole. Between 4 and 8 h post-infection, the DC develops into the non-infectious reticulate cell (RC) form, which replicates to yield a bacteria-filled inclusion called the *A. phagocytophilum*-occupied vacuole (ApV). From 8 to 20 h, the intravacuolar population consists exclusively of replicating RC bacteria. Conversion back to the DC form occurs between 28 and 32 h. DC organisms exit host cells between 28 and 36 h to initiate the next round of infection (Troese and Carlyon, 2009). Host–pathogen interactions that are critical for RC-to-DC transition are unknown.

Microbial acquisition of host nutrients is essential for the development of infectious disease. This is especially important for obligate intracellular pathogens whose reduced genomes render them auxotrophic for many metabolites and imposes a reliance on host cell nutrients. *A. phagocytophilum* satisfies this need, at least in part, by redirecting vesicular traffic to the ApV (Xiong *et al*., 2009; Huang *et al*., 2010a; Niu *et al*., 2012; Xiong and Rikihisa, 2012). Rab GTPases regulate membrane dynamics and route vesicular traffic in eukaryotic cells. Rabs cycle between two distinct states: a cytosolic, inactive guanosine diphosphate (GDP)-bound form and a membrane-associated, active guanosine triphosphate (GTP)-bound form that directs vesicular trafficking and membrane fusion events (Stenmark, 2009). We previously demonstrated that several green fluorescent protein (GFP)-tagged Rabs are specifically recruited to the ApV. Of these, GFP-Rab10 localizes to the ApV in an atypical, guanine nucleotide-independent manner, suggesting that the bacterium actively targets Rab10-positive vesicles (Huang *et al*., 2010a). Rab10 directs exocytic traffic from the *trans*-Golgi network (TGN) (Liu and Storrie, 2012). The significance of Rab10 to *A. phagocytophilum* pathobiology is unknown.

Herein, we provide evidence that Rab10-positive TGN vesicles are routed to and delivered into the ApV in a Rab10-dependent manner. In agreement with this observation, lipidomic analysis revealed that the pathogen incorporates sphingolipids. Rab10-dependent TGN vesicle import into the ApV is critical for bacterial transcriptional up-regulation of a marker of RC-to-DC transition and infectious progeny generation. The *A. phagocytophilum* surface protein, uridine monophosphate kinase (UMPK), was identified as a guanine nucleotide-independent Rab10-specific ligand. Overall, this report demonstrates that Rab10 is important for *A. phagocytophilum* TGN parasitism and completion of the pathogen's biphasic infection cycle and advances understanding of the diverse ways by which intracellular bacteria exploit Rab GTPases and membrane traffic.

Results

Endogenous and ectopically expressed Rab10 localize to the *A. phagocytophilum*-occupied vacuolar membrane and with intravacuolar *A. phagocytophilum* organisms

To determine if GFP-Rab10 localizes to the ApV in a host cell type besides myeloid cells (Huang *et al.*, 2010a), we assessed for the phenomenon in infected RF/6A endothelial cells using laser scanning confocal microscopy (LSCM). RF/6A cells were also selected for this purpose because, in addition to being permissive for *A. phagocytophilum* infection, they are large and flat, which makes them ideal for imaging the ApV (Munderloh *et al.*, 2004; Sukumaran *et al.*, 2011; Beyer *et al.*, 2014). Similar to that previously observed for infected HL-60 cells (Huang *et al.*, 2010a), GFP-Rab10-positive vesicles surrounded ApVs (Fig. 1A). Additionally, GFP-Rab10 was observed within ApVs encircling *A. phagocytophilum* organisms. GFP alone remained diffuse in the cytosol of infected cells. Given these observations for GFP-Rab10, we hypothesized that endogenous Rab10-positive vesicles are delivered into the ApV. Accordingly, we screened infected RF/6A cells with antibodies against endogenous Rab10 and the bacterial outer membrane protein (OMP), Asp14 (14 kDa *A. phagocytophilum* surface protein) (Kahlon *et al.*, 2013) or APH0032, which is a bacterial effector that is pronouncedly expressed late (24 to 32 h) during the infection cycle and localizes to the *A. phagocytophilum* occupied vacuolar membrane (AVM) (Huang *et al.*, 2010b). In addition to producing a vesicular labelling pattern in the cytosol and at the peripheries of ApVs, endogenous Rab10 signal surrounded individual intravacuolar bacteria in ring-like labelling patterns and partially colocalized with Asp14 signal (Fig. 1B and C). Z-stack analysis and three-dimensional (3D) rendering of a representative ApV confirmed the presence of Rab10-positive vesicles within the vacuole associated with intravacuolar bacteria (Fig. 1D and Movie S1). Thus, Rab10-positive vesicles are recruited to the ApV and delivered into its lumen where they associate with *A. phagocytophilum* organisms. Notably, a minor portion of APH0032-positive ApVs lacked lumenal Rab10 signal, as exemplified by the ApV in the lower-right corners of the images presented in Fig. 1C and D. This observation suggests that delivery of Rab10-positive vesicles into the ApV may be a temporal event that occurs during the period of APH0032 expression.

The ApV localizes adjacent to the Golgi apparatus and TGN-derived vesicles are delivered into its lumen where they associate with *A. phagocytophilum* organisms

Given that Rab10 directs exocytic traffic from the TGN, we investigated if the ApV associates with the Golgi apparatus and if the Rab10-positive vesicles delivered into its lumen are TGN derived. Screening *A. phagocytophilum* infected RF/6A cells with antibodies against markers for the *cis*-Golgi (GM130 and GolgB1), *medial*-Golgi (GolgB1) and *trans*-Golgi (TGN46) revealed ApVs closely apposed to and in many instances wrapped by the Golgi (Fig. 2). Signal for TGN46 but not GM130 or GolgB1 was detected within ApV lumens, indicating specific delivery of TGN-derived vesicles or fragments. TGN46 labelling inside ApVs partially colocalized with Asp14 signal (Fig. 3A). Z-stack imaging and 3D rendering of a representative ApV further verified that the presence of TGN46-positive vesicles closely associated with intravacuolar *A. phagocytophilum* organisms (Fig. 3B and C and Movie S2) and was highly similar to the observed proximal association of Rab10-positive vesicles near the surfaces of the bacteria (Fig. 1B–D and Movie S1). As a

complementary approach, organelles from uninfected and *A. phagocytophilum*-infected HL-60 cells were fractionated using a density gradient centrifugation method that keeps the ApV intact (Niu *et al*., 2012). Immunoblot analysis revealed altered distribution of TGN46 in the fractions of infected versus uninfected cells (Fig. 3D). Specifically, TGN46 co-migrated to the fraction in which the *A. phagocytophilum* OMP, P44 (Truchan *et al*., 2013), was most abundant.

Given the abundance of TGN vesicles/fragments delivered into the ApV, we examined Golgi integrity during *A. phagocytophilum* infection. ApVs were demarcated using an antibody against the cytoskeletal protein, vimentin, which localizes to the AVM (Sukumaran *et al*., 2011). In uninfected host cells and host cells with low *A. phagocytophilum* loads (one to three ApVs per cell), the Golgi remained intact, and intravacuolar bacteria were TGN46 positive (Fig. S1A and B). However, bacterial load-dependent fragmentation of the Golgi was observed for cells having medium (4–10 ApVs per cell) and high bacterial loads (≥ 11 ApVs per cell) (Fig. S1B). Additionally, even though the *cis*-Golgi, *medial*-Golgi and *trans*-Golgi were each fragmented and dispersed throughout host cells with high bacterial loads, only a TGN46 signal was detected within ApVs (Fig. S1B and C). This finding reinforces that *A. phagocytophilum* selectively targets TGN-derived exocytic traffic. Furthermore, in cells with high *A. phagocytophilum* loads, not all of the ApV lumens were visually TGN46 positive (Fig. S1B), which is likely due to the bacterial demand for TGN vesicles exceeding the supply. Collectively, these data support the findings that the ApV interacts with the Golgi apparatus and intercepts TGN-derived traffic and that TGN-derived vesicles or fragments are delivered into the ApV lumen.

Structured illumination microscopic analyses confirm that Rab10-positive and TGN46-positive vesicles are present in the ApV associated with intravacuolar *A. phagocytophilum* organisms

The partial colocalization of Rab10 and TGN46 signals with Asp14-associated and 4′,6-diamidino-2-phenylindole (DAPI)-associated signals of *A. phagocytophilum* observed using LSCM suggested that Rab10-positive *trans*-Golgi-derived vesicles are present within the ApV lumen in close proximity to intravacuolar *A. phagocytophilum* bacteria. LSCM has a lateral resolution of approximately 200 nm (Allen *et al*., 2014). Within cells, and presumably within the ApV, macro-molecular associations occur in spatial distances less than 200 nm. Therefore, structured illumination microscopy, a form of super-resolution microscopy, which has a lateral resolution of approximately 100 nm (Allen *et al*., 2014), was employed to more accurately gauge whether Rab10 and TGN46 signals were associated with intravacuolar *A. phagocytophilum* organisms. Supporting the phenomena observed via LSCM, SIM imaging revealed the Rab10 signal to exhibit a vesicle-like pattern that was diffuse in the host cell cytosol and a more clustered pattern that partially localized with Asp14-positive and DAPI-positive *A. phagocytophilum* organisms (Fig. 4A). Likewise, the TGN46 signal pronouncedly colocalized with bacterial-associated Asp14 and DAPI signals (Fig. 4B). These data indicate that Rab10 and TGN46 are within 100 nm of the surfaces of *A. phagocytophilum* organisms.

Sphingolipids are delivered into the ApV and incorporated by *A. phagocytophilum*

Anaplasma phagocytophilum lacks genes that are necessary for sphingolipid synthesis (Dunning Hotopp *et al.*, 2006). Given that the TGN is enriched in sphingolipids (van Meer, 1998) and TGN vesicles accumulate in the ApV, we examined for the delivery of sphingolipids into the ApV lumen using BODIPY Texas Red (TR) ceramide. This fluorescently labelled lipid accumulates in the Golgi, where it is modified into fluorescently labelled sphingolipids that subsequently traffic to the plasma membrane via TGN-derived secretory vesicles (Pagano *et al.*, 1991). Infected host cells were incubated with BODIPY TR ceramide and examined using LSCM. BODIPY TR ceramide-positive vesicles were observed surrounding ApVs and within ApV lumen associating with bacteria in ring-like labelling patterns (Fig. 5A). Because the infection was asynchronous and all *A. phagocytophilum* bacteria were TR positive, we inferred that BODIPY TR-derived sphingolipids associated with both RC and DC forms. Furthermore, ultra performance liquid chromatography–electrospray ionization–tandem mass spectrometry (UPLC-ESI-MS/MS) analyses detected the presence of multiple ceramide, sphingomyelin and monohexyl sphingolipid subspecies in *A. phagocytophilum* DC organisms that had been naturally released from infected HL-60 cells, but not in media from uninfected control HL-60 cells (Fig. 5B–E). These results substantiate that host cell sphingolipids that are typically found in the TGN are delivered into the ApV lumen and are incorporated by *A. phagocytophilum*.

Anaplasma phagocytophilum acquisition of Rab10-positive TGN vesicles precedes conversion to the infectious DC form

To better understand the relevance of Rab10-positive TGN vesicle delivery to *A. phagocytophilum* intracellular development, we examined if the vesicles specifically associate with the DC or RC form. Infected RF/6A cells were screened with Rab10 or TGN46 antibody together with an antibody against the *A. phagocytophilum* DC-specific protein, APH1235 (Troese *et al.*, 2011; Mastronunzio *et al.*, 2012). An RC-specific marker has yet to be identified. As previously reported (Troese *et al.*, 2011; Mastronunzio *et al.*, 2012), APH1235-positive *A. phagocytophilum* organisms were detected bound to host cell surfaces and as intracellular clusters, presumably within vacuoles (Fig. 6A). Strikingly, Rab10 and TGN46 were nearly undetectable on APH1235-positive bacteria. This observation indirectly suggests that RC but not DC organisms predominantly associate with TGN vesicles.

To further investigate this phenomenon, we assessed Rab10 and TGN46 localization within infected cells by LSCM over a 36 h synchronized infection time course. We used LSCM to examine APH0032 and APH1235 expression kinetics to verify that the infection cycle proceeded as expected. APH0032 expression/AVM localization was examined for the additional reason that one of our initial experiments suggested that Rab10 vesicle import into the ApV is a temporal event that occurs coincident with APH0032 expression (Fig. 1C and D). Consistent with previous observations (Huang *et al.*, 2010b), the percentages of APH0032-positive AVMs pronouncedly rose from 8 to 28 h (Fig. 6B and C). Also as previously reported (Troese *et al.*, 2011; Mastronunzio *et al.*, 2012), the percentages of *A. phagocytophilum* organisms expressing APH1235 dropped from 100% at 4 h to nearly 0% between 12 and 24 h and then pronouncedly increased again to more than 80% by 36 h (Fig.

6C). The localization of TGN46 and Rab10 around and within ApVs occurred synchronously. Rab10-positive vesicles and TGN vesicles were detected surrounding ApVs beginning at 16 h (Fig. 6B and C). Both markers were observed within ApVs beginning at 24 h and peaked at 28 h, a time point at which nearly 100% of ApVs were Rab10 and TGN46 positive. After 28 h, intravacuolar Rab10 and TGN46 signals waned considerably. Notably, the time points at which Rab10 and TGN46 signals associated with the ApV and *A. phagocytophilum* organisms preceded those when the bacteria were APH1235 positive. The coincident and temporal associations of Rab10 and TGN46 signals with *A. phagocytophilum* organisms indirectly suggested that Rab10 and TGN46 antibodies did not non-specifically label the bacteria. To verify that this was the case, host cell-free RC and DC organisms were screened via LSCM. Both RCs and DCs were stained by DAPI and labelled by P44 antibody (Fig. S2). Rab10 and TGN46 antibodies labelled only the RC morphotype. Collectively, these data demonstrate that delivery of Rab10-positive TGN vesicles into the ApV and their association with intravacuolar bacteria precedes *A. phagocytophilum* conversion from the replicative RC form to the infectious DC form.

Knockdown of Rab10 markedly reduces both TGN vesicle delivery into the ApV and infection

To define the significance of Rab10 to *A. phagocytophilum* TGN parasitism, we assayed for TGN vesicle recruitment to and delivery into the ApV in infected host cells in which Rab10 had been knocked down. For this experiment, we used HEK-293T cells because they are susceptible to *A. phagocytophilum* infection and have a high transfection efficiency (≥ 75%) relative to RF/6A and HL-60 cells (<20%) (Beyer *et al.*, 2014). Furthermore, GFPR-ab10 and TGN46 localize to and within the ApV, respectively, in these cells (Fig. S3A and B). HEK-293T cells were treated with small interfering RNA (siRNA) targeting Rab10, glyceraldehyde 3-phosphate dehydrogenase (GAPDH) or non-targeting siRNA. Knockdown of target protein expression was confirmed by Western blot (Fig. 7A). Rab10 knockdown had no effect on Golgi apparatus integrity, as TGN46 labelling revealed the organelle to be perinuclear, condensed and structurally intact (Fig. S3C). Treated cells were infected with *A. phagocytophilum* followed by LSCM examination. The percentage of ApVs with lumenal TGN46 signal was reduced by approximately fourfold in Rab10 siRNA-targeting versus non-targeting siRNA-treated HEK-293T cells (Fig. 7C). Also, whereas the Golgi apparatus was fragmented and barely detectable in infected control cells, it remained intact in infected cells in which Rab10 had been knocked down (Fig. 7B). Furthermore, the percentage of infected cells and the number of ApVs per cell were reduced by approximately twofold and threefold, respectively, in Rab10-knockdown cells compared with control cells (Fig. 7D and E). Taken together, these data suggest that Rab10 is critical for TGN recruitment to the ApV, for TGN vesicle uptake by the ApV and for productive *A. phagocytophilum* infection.

Rab10-dependent acquisition of TGN vesicles is important for the generation of infectious DC progeny

Because the *A. phagocytophilum* load was pronouncedly reduced in host cells in which Rab10 had been knocked down (Fig. 7D and E), yet many of these cells were observed to harbour numerous late-stage ApVs (Fig. 7B), we reasoned that acquisition of Rab10-positive TGN vesicles was not important for bacterial replication but was instead critical for the

production of infectious progeny. To test this hypothesis, media from *A. phagocytophilum*-infected HEK-293T cells that had been treated with Rab10, GAPDH or non-targeting siRNA was collected at 48 h post-infection and added to naïve cells. In untreated cells, this media contains naturally liberated, infectious *A. phagocytophilum* DC organisms (Beyer *et al*., 2014). If siRNA treatment inhibited RC-to-DC conversion, then fewer DC bacteria would be released into the media and, consequently, would produce a lower level of infection in recipient cells. At 24 h, the percentage of infected host cells and the number of ApVs per cell was more than twofold and nearly fourfold lower, respectively, in cells that had been incubated with media from infected Rab10-knockdown cells relative to those that had received media from infected non-targeting siRNA-treated control cells (Fig. 8A and B). To confirm that Rab10 knockdown inhibited RC-to-DC transition, the experiment was repeated and quantitative reverse transcription (qRT)-PCR was performed on RNA collected at 24, 28 and 32 h post-inoculation to assess for *aph1235* expression. The selected time points are those during which *A. phagocytophilum* TGN acquisition, *aph1235* up-regulation (Troese *et al*., 2011;Mastronunzio *et al*., 2012) and RC-to-DC transition (Troese and Carlyon, 2009) would normally occur. As expected (Troese *et al*., 2011; Mastronunzio *et al*., 2012), *aph1235* expression rose over the time course in host cells that had been treated with non-targeting siRNA (Fig. 8C). In contrast, *aph1235* transcript levels did not increase at any time point in host cells in which Rab10 had been knocked down. Thus, Rab10-dependent acquisition of TGN vesicles is critical for *aph1235* up-regulation, RC-to-DC conversion and the production of *A. phagocytophilum* infectious progeny.

Identification of an *A. phagocytophilum* Rab10-specific ligand

Because Rab10-positive vesicles are recruited to the ApV in a guanine nucleotide-independent, tetracycline-sensitive manner (Huang *et al*., 2010a) and are delivered into the lumen where they associate with *A. phagocytophilum* organisms, we reasoned that at least one pathogen-encoded protein contributes to these processes. To identify potential *A. phagocytophilum* Rab10-interacting proteins, we incubated whole-cell lysates of infected and uninfected HL-60 cells with glutathione sepharose beads coated with glutathione-*S*-transferase (GST)-tagged Rab10 or GST alone. A 26 kDa protein that was specifically isolated from infected cells by the GST-Rab10 beads (Fig. 9A) was identified by mass spectrometry as APH0111 (Fig. 9B). This protein is annotated as UMPK (Dunning Hotopp *et al*., 2006), a nucleotide scavenger enzyme that catalyses the conversion of uridine monophosphate to uridine diphosphate (Yan and Tsai, 1999). To validate that UMPK and Rab10 interact and to evaluate the specificity of the interaction, whole-cell lysates of *Escherichia coli* expressing Halo-tagged UMPK were incubated with beads coated with GST alone, GST-Rab10, GST-Rab11 or GST-Rab35. Rab11 and Rab35 were included because they also localize to the AVM (Huang *et al*., 2010a). Only GST-Rab10-coupled beads precipitated recombinant UMPK (Fig. 10A).

To assess if UMPK colocalizes with Rab10 in living cells and in a guanine nucleotide-independent manner, HeLa cells were cotransfected to express Halo-UMPK and GFP-tagged wild-type Rab10, GTP-locked Rab10Q68L, GDP-locked Rab10T23N or guanine nucleotide binding defective Rab10N122I and examined by LSCM. HeLa cells coexpressing Halo-UMPK and GFP alone or one of several additional GFP-tagged Rabs that are known to be

recruited to the ApV (Rab1A, Rab4A, Rab11A, Rab14, Rab22A and Rab35) or not (Rab5 and Rab7) (Huang *et al*., 2010a) served as controls. Consistent with the guanine nucleotide-independent specificity of UMPK for Rab10, coexpression of Halo-UMPK with each GFP-tagged Rab10 isoform yielded aggregative vesicular labelling patterns where Halo and GFP signals completely overlapped (Fig. 10B). Of the other Rab GTPases, Halo-UMPK poorly localized with Rab35 and did not colocalize with any other Rab (Fig. 10B and C). Halo and GFP signals did not colocalize in cells that expressed either Halo alone and Halo-UMPK and GFP alone (Fig. S4A) or GFP-Rab10 (Fig. S4B). Halo-tagged *E. coli* UMPK and GFP-Rab10 also did not colocalize in transfected cells (Fig. S4C), further indicating the specificity of the *A. phagocytophilum* UMPK-Rab10 interaction. To confirm that UMPK is capable of binding Rab10 in living cells, Halo-UMPK was coexpressed with and assessed for the ability to precipitate GFP-tagged Rab10 isoforms. All GFP-tagged Rab10 isoforms, but neither GFP nor GFP-Rab7, coprecipitated with Halo-UMPK (Fig. 10D). Taken together, these data identify *A. phagocytophilum* UMPK as a Rab10-specific ligand that binds the GTPase in a guanine nucleotide-independent manner.

UMPK is an *A. phagocytophilum* surface protein

Uridine monophosphate kinase is a 244-amino-acid protein with a predicted molecular mass of 26 kDa and two transmembrane domains that putatively present amino acids 1 to 100 and 155 to 244 on the bacterial surface (Figs 9B and 11A and B). Our previous evaluation of the *A. phagocytophilum* surface proteome identified UMPK as a likely surface protein (Kahlon *et al*., 2013). Mining the UMPK tryptic peptides recovered in that study (Kahlon *et al*., 2013) revealed that they mapped to the protein's two predicted surface-exposed regions (Fig. 9B). To verify that UMPK is a surface protein, *A. phagocytophilum*-infected RF/6A cells and human neutrophils were screened with antibody specific for a peptide corresponding to predicted surface-exposed UMPK residues, 189–195 (Figs 9B, 11A and B and S5A), together with APH0032 antibody. In both infected host cell types, $UMPK_{182–195}$ antibody labelled intravacuolar bacteria, but not the APH0032-positive AVM (Fig. 11C). Next, to determine if UMPK residues 182–195 are an immunoaccessible domain that is exposed on the bacterial outer membrane, the surfaces of intact host cell-free *A. phagocytophilum* organisms were treated with proteinase K, a proven approach for verifying surface presentation of *A. phagocytophilum* and *Chlamydia trachomatis* OMPs (Wang *et al*., 2006; Ojogun *et al*., 2012; Kahlon *et al*., 2013; Seidman *et al*., 2014). Western-blotted lysates of proteinase K-treated and vehicle-treated DC bacteria were screened with $UMPK_{182–195}$ antiserum. Positive control antiserum targeted a confirmed surface-exposed epitope of Asp55 (55 kDa *A. phagocytophilum* surface protein) (Ge and Rikihisa, 2007), while negative control antiserum targeted APH0032, which is not an OMP (Huang *et al*., 2010b). Following surface proteolysis, neither $UMPK_{182–195}$ nor Asp55 was detected (Fig. 11D). APH0032 was amply detected in lysates of both treated and vehicle control-treated bacteria. Immunofluorescence examination of *A. phagocytophilum*-infected host cells at multiple time points post-infection revealed that the bacterium constitutively expressed UMPK (Fig. S5B). Thus, UMPK is an *A. phagocytophilum* surface-localized Rab10-specific ligand that is expressed throughout the course of infection.

Discussion

Abu Kwaik and Bumann (2013) coined the term, 'nutritional virulence' to describe the phenomenon that, without access to host nutrients, microbial pathogens cannot survive and cause disease. This study provides important insights into how *A. phagocytophilum* satisfies its nutritional virulence requirements, specifically host–pathogen interactions that are critical for it to complete its biphasic developmental cycle and yield infectious progeny. Figure 12 presents our hypothetical model for these findings as follows. After *A. phagocytophilum* has entered its host cell, transitioned from the DC to the RC form and begun dividing, the ApV localizes to and is wrapped by the Golgi apparatus. During the period of expansive bacterial replication, which occurs between 12 and 28 h, *A. phagocytophilum* targets TGN exocytic traffic in a Rab10-dependent manner. Hijacked Rab10-positive TGN vesicles localize to and within the ApV. Within the ApV lumen, the bacterium acquires sphingolipid-rich contents of the imported TGN vesicles and reconverts to its infectious DC form.

Rab10 is important for RC-to-DC conversion. APH1235 contributes to invasion of mammalian host cells (Mastronunzio *et al*., 2012), is up-regulated during RC-to-DC transition (Troese *et al*., 2011) and is therefore a marker for the expression profile associated with the generation of infectious progeny. Rab10 knockdown in host cells did not affect bacterial replication but impeded TGN vesicle import into the ApV, *aph1235* expression and the generation of DC bacteria. In addition to TGN vesicles, *A. phagocytophilum* also promotes delivery of autophagic bodies into the ApV lumen as a major amino acid source (Niu *et al*., 2012). However, autophagy does not involve Rab10, and autophagosome recruitment would likely not be affected in Rab10 siRNA-treated cells. Thus, while autophagy is important for intracellular growth, it may not be involved in generating infectious progeny. *A. phagocytophilum* organisms that are positive for Rab10 and TGN46 are APH1235 negative and vice versa, suggesting that the bacterium incorporates/utilizes TGN vesicle contents before RC-to-DC conversion occurs. The pathogen may use TGN vesicle contents to compensate for its auxotrophies and as carbon sources to fuel the energy demand associated with the RC-to-DC switch.

Many intracellular bacteria parasitize host cell lipids (reviewed by Vromman and Subtil, 2014). *C. trachomatis* was the first bacterium shown to recruit the Golgi apparatus and to deliver both ceramide and cholesterol into the lumen of its inclusion (Hackstadt *et al*., 1995, 1996; Scidmore *et al*., 1996; Wolf and Hackstadt, 2001; Carabeo *et al*., 2003; Heuer *et al*., 2009). *C. trachomatis* hijacks the TGN by targeting Rab6, Rab11 and Rab14 (Rzomp *et al*., 2003; Lipinski *et al*., 2009; Capmany and Damiani, 2010), whereas *A. phagocytophilum* does so by co-opting Rab10. *A. phagocytophilum* acquires endogenous host cell and BODIPY TR-labelled sphingolipids, the latter of which would have been derived from precursor BODIPY TR ceramide and produced in the TGN. Because both RC and DC forms were BODIPY TR positive and lipidomics revealed that naturally liberated DC bacteria were enriched in sphingolipids, we infer that DC organisms retain TGN-derived sphingolipids assimilated during the RC stage. How this occurs is unknown. The close apposition of TGN vesicles with intravacuolar *A. phagocytophilum* organisms could allow for lipid transfer proteins, which are present in TGN vesicle membranes and mediate lipid exchange between donor and acceptor membranes (Lev, 2010; Blom *et al*., 2011), to deliver host-derived

sphingolipids to the bacterium. Such sphingolipids may help stabilize the *A. phagocytophilum* peptidoglycan-deficient cell wall, as a similar role has been established for cholesterol (Lin and Rikihisa, 2003).

The Golgi is destabilized to the point that it is barely detectable in host cells with high *A. phagocytophilum* burdens. This alters neither Rab10 ApV localization nor bacterial replication, as both proceed equally as well in host cells treated with the Golgi destabilizing agent, brefeldin A, or vehicle control (Mott *et al.*, 1999; Huang *et al.*, 2010a). Golgi fragmentation does not occur in cells with lower loads likely because the bacterial demand does not exceed the rate at which the organelle is replenished. Under high *A. phagocytophilum* load, however, the demand is too high to allow for Golgi replenishment, which results in destabilization of the organelle. Based on GM130 (*cis*-Golgi marker) labelling, a previous report noted that Golgi destabilization occurred in host cells heavily infected with *A. phagocytophilum* (Xiong and Rikihisa, 2012). Because this study did not label for the TGN (Xiong and Rikihisa, 2012), it could not determine the fate of TGN-derived vesicles and their relevance to *A. phagocytophilum* infection.

In terms of pathogen–Rab interactions, it is well documented that bacterial manipulation of Rabs can culminate in SNARE-mediated fusion of the routed vesicles with the pathogen-occupied vacuolar membrane. This, in turn, transports vesicle contents into the lumen for bacterial use (Arasaki *et al.*, 2012; Sherwood and Roy, 2013). A lesser-understood phenomenon that also occurs and for which evidence has only recently begun to accumulate is the transport of entire vesicles into pathogen-occupied vacuoles (POVs) in the absence of membrane fusion. Indeed, intact lipid droplets, peroxisomes, multivesicular bodies and endoplasmic reticulum-derived vesicles are delivered into the *C. trachomatis* inclusion (Beatty, 2006; Cocchiaro *et al.*, 2008; Dumoux *et al.*, 2012; Boncompain *et al.*, 2014). Also, Rab14, which like Rab10 directs TGN exocytic traffic (Junutula *et al.*, 2004), was detected within the *C. trachomatis* inclusion (Capmany and Damiani, 2010). Until this report, import of host cell-derived vesicles into a POV had not been observed for another vacuole-adapted intracellular bacterium besides *C. trachomatis*. How intracellular bacteria orchestrate membrane fusion-independent delivery of Rab-decorated vesicles into the POV lumen is undefined. Notably, it was recently demonstrated that two secreted proteins of the protozoan pathogen, *Toxoplasma gondii*, localize to and function synergistically to mediate passive transfer of small molecules across the parasitophorous vacuole membrane (Gold *et al.*, 2015).

Anaplasma phagocytophilum UMPK is a novel bacterial Rab ligand that specifically binds Rab10 in a guanine nucleotide-independent manner, which suggests that it interacts with a region of Rab10 that is unaltered by its guanine nucleotide-bound status. UMPK's annotated function in pyrimidine biosynthesis (Yan and Tsai, 1999) and its role in engaging Rab10 demonstrated herein categorize it as a moonlighting protein, or a protein that performs multiple autonomous, unrelated functions (Henderson and Martin, 2011, 2013). There are over 200 examples of bacterial metabolic proteins and chaperones functioning as virulence factors (Henderson and Martin, 2011, 2013). As typified by *A. phagocytophilum* UMPK, which is present on the bacterium's surface, these proteins often execute their virulence functions at sites that are topologically distinct from their housekeeping roles (Henderson

and Martin, 2011, 2013). *E. coli* UMPK is a moonlighting protein that localizes not only to the cytoplasm where it functions as both a nucleotide scavenger enzyme and a transcriptional regulator but also to the outer membrane where it performs an unknown function (Kholti *et al.*, 1998; Landais *et al.*, 1999). Also, *Yersinia pestis* cytidine monophosphate kinase, a UMPK homolog, makes an undefined contribution to virulence (Walker *et al.*, 2012).

Based on UMPK's surface presentation and the proximity of Rab10-positive TGN vesicles to bacteria in the ApV lumen, it will be important to investigate if UMPK binds Rab10 as a receptor on the newly imported vesicles to promote utilization of their contents. However, because a reliable system for performing knockout complementation studies in *A. phagocytophilum* is currently lacking, this hypothesis cannot yet be evaluated. As important progress towards effective systems for assessing *bona fide* gene function in obligate intracellular bacteria continues to be made (Mishra *et al.*, 2012; Cheng *et al.*, 2013; Beare and Heinzen, 2014; Wood *et al.*, 2014), we anticipate that it will be possible to validate *A. phagocytophilum* UMPK's role during infection in the near future.

Obligate intracellular bacteria cause infections that can be debilitating, chronic and even fatal. Because they must parasitize nutrients from their hosts to survive, understanding their nutritional virulence strategies may elucidate new treatment options. This study indicates *A. phagocytophilum* Rab10-dependent TGN parasitism could potentially be targeted as a novel therapeutic. Accordingly, it will be important to assess for translocation of intact vesicles into the POVs of other intracellular bacterial species and to ultimately determine if UMPK or other bacterial surface proteins mediate interactions with the delivered vesicular cargo.

Experimental procedures

Cultivation of uninfected and *A. phagocytophilum*-infected host cell lines and neutrophils

Uninfected and *A. phagocytophilum* (NCH-1 strain)-infected human promyelocytic HL-60 cells [CCL-240; American Type Culture Collections (ATCC), Manassas, VA] and RF/6A rhesus monkey choroidal endothelial cells (CRL-1780; ATCC) were cultured as described previously (Huang *et al.*, 2010b). HeLa 229 epithelial cells (CCL-1.2; ATCC) were grown in Roswell Park Memorial Institute 1640 (Invitrogen, Carlsbad, CA) supplemented with 10% foetal bovine serum (FBS; Gemini Bio-Products, Sacramento, CA) at 37°C with 5% CO_2. HEK-293T cells were cultured in Dulbecco's modified Eagle's medium with L-glutamine, 4.5 g l^{-1} of D-glucose and 100 mg l^{-1} of sodium pyruvate (Invitrogen) supplemented with 10% FBS, 1× minimal essential medium non-essential amino acids (Invitrogen) and 15 mM of HEPES (Affymetrix, Cleveland, OH) at 37°C with 5% CO_2. Human neutrophils were isolated from peripheral blood from healthy donors using Polymorphprep (Axis-Shield; Greiner Bio-One, Frickenhausen, Germany) as described previously (Carlyon *et al.*, 2004). The protocol (HM11407) for obtaining donor blood for the purpose of isolating neutrophils has been reviewed and approved by the Virginia Commonwealth University Institutional Review Board with respect to scientific content and compliance with applicable research and human subjects regulations.

Plasmids

Previously described constructs encoding GFP-tagged and GST-tagged Rab proteins were kind gifts from Marci Scidmore (Cornell University) and have been described previously (Rzomp *et al.*, 2003; Cortes *et al.*, 2007; Huang *et al.*, 2010a). APH0111 (UMPK) DNA was synthetically generated and cloned into the SgfI and PmeI sites of the pFN21K vector mammalian expression vector by Promega Corporation (Madison, WI). The insert was subcloned into the SgfI and PmeI sites of the *E. coli* expression vector pFN18A (Promega) using the Flexi system transfer kit (Promega). The pFN21K control vector that was used for expressing the Halo tag alone was constructed by digesting the original pFN21K vector with SgfI and PmeI to remove the barnase gene. The digested vector was religated with a double-stranded DNA bridge that was generated using oligonucleotides 5′-CGCGTAAGGGTAGGTTT-3′ (sense strand) and 5′-AAACGTACCCTTACGCGAT-3′ (antisense strand). DNA encoding the *E. coli* UMPK gene was amplified from Alpha-Select Gold Efficiency *E. coli* (Bioline, Taunton, MA) using primers 5′-*ATAT*GCGATCGCCGCTACCAATGCAAAACCCGTCTATAAACGCATTC-3′ (sense strand; spacer nucleotides are italicized; SgfI site is underlined) and 5′-*AACT*GTTTAAACTTATTCCGTGATTAAGTCCCTTCTTTTTCACC-3′ (antisense strand; spacer nucleotides are italicized; PmeI site is underlined) and cloned into the SgfI and PmeI sites of the pFN21K. DNA encoding the *A. phagocytophilum* UMPK gene was amplified from NCH-1 DNA using primers 5′-*GACC*GCGATCGCCGATTGTAATGTTGTGGAGAATGTGCGTTATTCTA-3′ (sense strand; spacer nucleotides are italicized; SgfI site is underlined) and 5′-*GTCG*GTTTAAACCTATCCAGATATAGTAGTAAACGTACCCC-3′ (antisense strand; spacer nucleotides are italicized; PmeI site is underlined) and ligated into pFN21K or pFN18A. All inserts were amplified with Platinum Pfx DNA polymerase (Invitrogen, Grand Island, NY), and the sequences verified by DNA sequencing.

GST-Rab10-mediated precipitation of endogenous UMPK

BL21 *E. coli* (Novagen, EMD Millipore, Billerica, MA) transformed with a plasmid encoding GST-Rab10 were grown to an optical density at 600 nm of 0.4 and induced with 100 μM of isopropyl β-D-1-thiogalactopyranoside at 16°C for 16 h. GST-Rab10 was solubilized from inclusion bodies using 1% sarkosyl in Brymora bacterial lysis buffer [10 mM Tris–HCl (pH 7.4), 250 mM NaCl, 1% (vol/vol) Triton x-100, 2.5 mM $MgCl_2$] and combined with the soluble fraction. GST-Rab10 was immobilized on glutathione sepharose beads (GE Healthcare Life Sciences, Little Chalfont, UK) with the addition of 2% Triton X-100 and 20 mM 3-[(3-cholamidopropyl)dimethylammonio]-1-propanesulfonate. Fifty million uninfected or *A. phagocytophilum*-infected HL-60 cells were lysed in radioimmunoprecipitation assay buffer [10 mM Tris-Cl (pH 8.0), 1 mM EDTA, 1% Triton X-100, 0.1% sodium deoxycholate and 140 mM NaCl]. The lysates were pre-cleared with glutathione beads to eliminate non-specific binding and then mixed with 5 mg of GST or GST-Rab10 glutathione beads for 2 h at 4°C. The beads were washed and boiled, and the eluates were resolved on a 20 cm acrylamide tris-glycine 10–20% gradient gel (Jule Inc., Milford, CT) using the Protean II XL Cell electrophoresis rig (BioRad, Hercules, CA). The gel was stained with SYPRO Ruby (Invitrogen). The approximately 26 kDa band of interest that was exclusively recovered from the *A. phagocytophilum*-infected host cell lysate was

excised and submitted to the W. M. Keck Facility at Yale University (New Haven, CT) for mass spectroscopy and database searching.

Immunofluorescence assays and microscopy

Cells for immunofluorescence assays were grown and infected on #1½ 12 × 12 mm glass coverslips for LSCM (Electron Microscopy Sciences, Hatfield, PA) or #1½ HP (i.e. 0.17 ± 0.005 mm thick) high-performance glass coverslips (Zeiss, Thornwood, NY) for SIM. They were fixed in 4% paraformaldehyde (Electron Microscopy Sciences) for 30 min followed by permeabilization with 0.5% Triton X-100 for 10 min and washed in 1× phosphate-buffered saline (PBS). In some cases, host cell-free *A. phagocytophilum* RC and/or DC organisms were recovered from infected HL-60 cells as described (Carlyon, 2005) and fixed to glass slides. The cells or host cell-free bacteria were screened with antibodies for immunofluorescence microscopy as previously described (Huang *et al.*, 2010c). Commercial primary antibodies were against TGN46 (Sigma-Aldrich, St. Louis, MO), GM130 (BD Biosciences, San Jose, CA), GolgB1 (Sigma-Aldrich), HaloTag (Promega), GFP (Invitrogen), Rab10 (Sigma-Aldrich) and vimentin (Abcam, Cambridge, MA). Antibodies against Asp14, APH1235, APH0032 and P44 were described previously (Huang *et al.*, 2010b; Troese *et al.*, 2011; Kahlon *et al.*, 2013). Affinity-purified rabbit polyclonal antiserum targeting a peptide corresponding to *A. phagocytophilum* UMPK amino acids 182 to 195 was generated by New England Peptide (Gardner, MA). Secondary antibodies conjugated to Alexa Fluor fluorochromes were obtained from Invitrogen. BODIPY ceramide/bovine serum albumin complex (Invitrogen) was added to infected RF/6A cells per manufacturer's instructions. Coverslips were mounted with Prolong Gold Anti-fade reagent with or without DAPI (Invitrogen). Images were obtained using an Olympus BX51 microscope affixed with a disc-spinning unit (Olympus, Center Valley, PA) or a Zeiss LSM 700 laser scanning confocal microscope. For SIM, coverslips were stained with 1 μg ml^{-1} of DAPI in 1× PBS for 5 min and mounted with Prolong Gold Anti-fade reagent without DAPI (Invitrogen). Images were obtained using a Nikon N-SIM superresolution microscope. LSCM and SIM were performed at the VCU Microscopy Facility, which is supported, in part, by funding from NIH-NINDS Center core grant (5P30NS047463) and NIH-NCI Cancer Center Support Grant (P30 CA016059). 3D movies were generated using Volocity Image Analysis Software (Perkin Elmer, Waltham, MA).

Colocalization studies

HeLa cells were seeded onto 12 × 12 mm coverslips (Electron Microscopy Sciences) and cotransfected with plasmid DNA encoding Halo alone, Halo-*A. phagocytophilum* UMPK, Halo-*E. coli* UMPK or GFP-UMPK, and various GFP-Rabs or GFP alone was processed and labelled using Lipofectamine 2000 (Invitrogen). HaloTag TMR Direct ligand (Promega) was added to wells containing cells transfected to express Halo-tagged protein. After 24 h, the cells were processed and labelled, where applicable, as described earlier, and examined by immunofluorescence microscopy for colocalization of Halo and GFP signals.

Infection assays

Neutrophils and HL-60 cells were infected with *A. phagocytophilum* DC organisms released from infected HL-60 cells by sonication as previously described (Troese and Carlyon, 2009).

RF/6A or HEK-293T cells were infected with *A. phagocytophilum* DC bacteria that had been naturally released from infected RF/6A cells into the culture media as follows. Adherent host cells to be infected were seeded onto 12 mm coverslips (Electron Microscopy Sciences) and overlain with 200 μl of *A. phagocytophilum*-laden media from heavily infected RF/6A cells. The supernatant was spun down on top of the cells at 1000 × *g* for 3 min followed by a 1 h incubation at 37°C with 5% CO_2. The cells were washed with 1× PBS to remove unbound bacteria, and fresh media was added. The cells were returned to 37°C with 5% CO_2 for 24 or 48 h or specific time points, after which the cells were fixed in 4% paraformaldehyde and examined by immunofluorescence microscopy.

Density gradient centrifugation

Uninfected or infected HL-60 cells of 2×10^7 were washed with ice-cold 1× PBS two times followed by one wash in cold homogenization buffer (HB; 250 mM sucrose, 10 mM Tris–HCl, pH 7.4,1 mM EDTA). The cells were suspended in 1 ml of cold HB with protease inhibitors (Roche) and transferred to a type B dounce homogenizer (Gerresheimer Kimble Chase LLC, Vineland, NJ). The cells were homogenized for 20 to 30 strokes until ≥ 90% of the host cells were lysed, as verified by the trypan blue exclusion assay. The homogenate was centrifuged at 500 × *g* for 5 min to pellet the nuclei and unbroken cells. The supernatant was overlain on top of a 5%, 15% or 25% continuous Opti-prep (Sigma-Aldrich) gradient. The gradient was centrifuged at 200,000 × *g* for 3 h in a Beckman Coulter (Indianapolis, IN) Optima XE-100 ultracentrifuge. Twelve 1 ml fractions were collected from the top of the gradient. Protein was concentrated from the fractions by trichloroacetic acid precipitation. Equal volumes of fractions 1 to 9 were immunoblotted using TGN46, GM130 and P44 antibodies.

Western blot analyses

Cell lysates or gradient centrifugation fractions were analysed by sodium dodecyl sulfate–polyacrylamide gel electrophoresis (SDS-PAGE) and Western blot as previously described (Troese *et al*., 2011). Commercially available primary antibodies targeted β-actin (Santa Cruz Biotechnology, Santa Cruz, CA), GAPDH (Sigma-Aldrich), GFP (Invitrogen), HaloTag (Promega), TGN46 (Sigma-Aldrich) and Rab10 (Sigma-Aldrich). Rabbit antisera against *A. phagocytophilum* proteins P44 (IJdo *et al*., 1999) and APH0032 (Huang *et al*., 2010b) were described previously. Rabbit antibody targeting a surface-exposed epitope of Asp55 (Ge and Rikihisa, 2007) was a kind gift from Yasuko Rikihisa (Ohio State University, Columbus, OH).

UPLC-ESI-MS/MS lipidomics of *A. phagocytophilum* DC organisms

Media from 3×10^7 *A. phagocytophilum*-infected (≥ 90%) HL-60 cells, which contained DC bacteria that had been naturally released, was spun at 300 × *g* twice to pellet host cells. The supernatant was spun at 1000 × *g* to remove host cellular debris. Next, the supernatant was spun at 5200 × *g* for 10 min to pellet DC organisms. The resulting pellet was washed twice with ice-cold PBS. All spins were performed at 4°C. As a background control, the media from 3×10^7 uninfected HL-60 cells was processed and analysed by UPLC-ESI-MS/MS in parallel. The *A. phagocytophilum* DC and control samples were examined for the presence of sphingolipids using UPLC-ESI-MS/MS as previously described (Simanshu *et*

al., 2013; Wijesinghe *et al*., 2014). Three separate biological replicates were examined in triplicate.

Rab10 siRNA knockdown

Seeded onto 12 mm glass coverslips (Electron Microscopy Sciences) were 4×10^5 HEK-293T cells. After 16 to 20 h, 80 μl of 5 μM ON-TARGETplus human Rab10 siRNA SMARTpool (GE Dharmacon, Lafayette, CO) was mixed with 320 μl of media and added to the wells. Non-targeting or GAPDH-targeting siRNA (GE Dharmacon) was added to control wells. After 72 h, 200 μl of media containing *A. phagocytophilum* DC organisms that had been released from infected RF/6A cells was added, and the bacteria were spun on the cells as described earlier. Additionally, cells from one well of each siRNA treatment were harvested for Western blot analysis to confirm knockdown. At 48 h post-infection, cells were harvested for quantitative PCR, processed for microscopy analyses, or the DC-laden media was added to naïve HEK-293T cells to detect the presence of infectious progeny.

Quantitative PCR and qRT-PCR

To analyse *A. phagocytophilum* load after siRNA treatment, DNA was isolated from host cells using the DNeasy Blood and Tissue Kit (Qiagen, Boston, MA). Fifty nanograms of DNA was analysed with primers specific for *A. phagocytophilum* 16S rDNA and host cell β-actin using SsoFast EvaGreen Supermix (BioRad) as previously described (Ojogun *et al*., 2012). To detect APH1235 transcript at 24, 28 and 32 h post-infection, cDNA was generated and analysed by qRT-PCR as previously described (Kahlon *et al*., 2013).

Precipitation of GFP-Rab10 proteins using Halo-UMPK

HeLa cells were seeded into a T-75 flask per pulldown and cotransfected with 12 μg each of Halo-UMPK (pFN21K) and GFP-Rab constructs using Lipofectamine 2000 (Invitrogen) per the manufacturer's instructions. After 24 h, the cells were trypsinized from the flask, spun down at 300 × *g* and subjected to one freeze–thaw cycle before complete lysis with Mammalian lysis buffer containing protease inhibitors (Promega). The pulldown was performed according to Promega's HaloTag Mammalian Pull-Down and Labeling Systems Technical Manual (TM#342) with the addition of 2.5 mM $MgCl_2$ in the binding and wash buffers. The eluates were resolved by SDS-PAGE, transferred to nitrocellulose and probed with GFP antibody (Invitrogen) as described (Troese *et al*., 2011).

Precipitation of Halo-UMPK by GST-Rab10 beads

BL21(DE3) *E. coli* (Novagen, EMD Millipore) transformed with the pFN18A Halo-UMPK construct were grown to an optical density at 600 nm of 0.4 and induced with 100 μM isopropyl β-D-1-thiogalactopyranoside at 25°C for 4 h. A culture of 50 ml culture was pelleted and lysed with Bugbuster (Novagen, EMD Millipore) containing EDTA-free Complete Protease Inhibitor (Roche, Indianapolis, IN). The lysate was divided equally, and each aliquot was incubated with 5 mg each of GST, GST-Rab10, GST-Rab11 or GST-Rab35 glutathione beads overnight on a rotator at 4°C. The beads were washed and boiled, and the eluates were resolved by SDS-PAGE and immunoblotted with HaloTag antibody (Promega).

Identification of UMPK as an *A. phagocytophilum* surface protein

Putative transmembrane domains in *A. phagocytophilum* UMPK were identified using TMPred (http://www.ch.embnet.org/software/TMPRED_form.html). Surface-exposed proteins of *A. phagocytophilum* DC organisms were removed by proteolysis as previously described (Ojogun *et al.*, 2012), except that the bacteria were treated with 4 mg ml^{-1} of proteinase K for 45 min at 25°C. We previously reported recovering UMPK as an *A. phagocytophilum* surface protein using a surface biotinylation-affinity chromatography approach (Kahlon *et al.*, 2013). To provide the previously unpublished sequences of the peptides recovered in this study, we mined the peptide spectra from this analysis and denoted them in Fig. S5.

Statistical analyses

One-way analysis of variance or Student's *t*-test was performed using the Prism 5.0 software package (GraphPad; San Diego, CA) to assess statistical significance as described. Statistical significance was set at $P \leq 0.05$.

Supplementary Material

Refer to Web version on PubMed Central for supplementary material.

Acknowledgments

We thank Yasuko Rikihisa (Ohio State University, Columbus, OH) for Asp55 antiserum and her and Qingming Xiong (Ohio State) for helpful advice on density gradient purification. We thank C. Dan Nacu of the Virginia Commonwealth University Department of Communication Arts and Design for producing the model in Fig. 12. We thank Bob Heinzen and Charles Larson for critical review of this manuscript, Scott Henderson for helpful discussions regarding SIM and Christine Van Duyn for technical assistance. This study was supported by funding from NIH grants AI072683 (to J. A. C.), HL125353 (to C. E. C.) and AI109068 (to C. E. C); National Center for Advancing Translational Sciences grant UL1TR000058 (to J. A. C.); the Veteran's Administration (VA Merit Review I BX001792 to C. E. C. and a Research Career Scientist Award 13F-RCS-002 to C. E. C.); the Israel Binational Science Foundation (BSF2011360 to C. E. C.); the Center for Clinical and Translational Research Endowment Fund of Virginia Commonwealth University (VCU) (to J. A. C.). LSCM and SIM were performed at the VCU Microscopy Facility, which is supported, in part, with funding from NIH-NINDS Center core grant 5P30NS047463 and NIH-NCI Cancer Center Support grant (P30 CA016059). VCU Lipidomics/Metabolomics Core services and products in support of the research project were generated, in part, by the VCU Massey Cancer Center with funding from NIH-NCI Cancer Center Support grant, P30 CA016059.

References

Abu Kwaik Y, Bumann D. Microbial quest for food *in vivo*: 'nutritional virulence' as an emerging paradigm. Cell Microbiol. 2013; 15:882–890. [PubMed: 23490329]

Allen JR, Ross ST, Davidson MW. Structured illumination microscopy for superresolution. Chem Phys Chem. 2014; 15:566–576. [PubMed: 24497374]

Arasaki K, Toomre DK, Roy CR. The *Legionella pneumophila* effector DrrA is sufficient to stimulate SNARE-dependent membrane fusion. Cell Host Microbe. 2012; 11:46–57. [PubMed: 22264512]

Beare PA, Heinzen RA. Gene inactivation in *Coxiella burnetii*. Methods Mol Biol (Clifton, NJ). 2014; 1197:329–345.

Beatty WL. Trafficking from CD63-positive late endocytic multivesicular bodies is essential for intracellular development of Chlamydia trachomatis. J Cell Sci. 2006; 119:350–359. [PubMed: 16410552]

Beyer AR, Truchan HK, May LJ, Walker NJ, Borjesson DL, Carlyon JA. The *Anaplasma phagocytophilum* effector AmpA hijacks host cell SUMOylation. Cell Microbiol. 2014; 17:504–519. [PubMed: 25308709]

Blom T, Somerharju P, Ikonen E. Synthesis and biosynthetic trafficking of membrane lipids. Cold Spring Harb Perspect Biol. 2011; 3:a004713. [PubMed: 21482741]

Boncompain G, Muller C, Meas-Yedid V, Schmitt-Kopplin P, Lazarow PB, Subtil A. The intracellular bacteria *Chlamydia* hijack peroxisomes and utilize their enzymatic capacity to produce bacteria-specific phospholipids. PLoS One. 2014; 9:e86196. [PubMed: 24465954]

Capmany A, Damiani MT. *Chlamydia trachomatis* intercepts Golgi-derived sphingolipids through a Rab14-mediated transport required for bacterial development and replication. PLoS One. 2010; 5:e14084. [PubMed: 21124879]

Carabeo RA, Mead DJ, Hackstadt T. Golgi-dependent transport of cholesterol to the *Chlamydia trachomatis* inclusion. Proc Natl Acad Sci U S A. 2003; 100:6771–6776. [PubMed: 12743366]

Carlyon JA. Laboratory maintenance of *Anaplasma phagocytophilum*. Current Protocols in Microbiology. 2005; Chapter 3(Unit 3A):2. [PubMed: 18770564]

Carlyon JA, Abdel-Latif D, Pypaert M, Lacy P, Fikrig E. *Anaplasma phagocytophilum* utilizes multiple host evasion mechanisms to thwart NADPH oxidase-mediated killing during neutrophil infection. Infect Immun. 2004; 72:4772–4783. [PubMed: 15271939]

Cheng C, Nair AD, Indukuri VV, Gong S, Felsheim RF, Jaworski D, et al. Targeted and random mutagenesis of *Ehrlichia chaffeensis* for the identification of genes required for *in vivo* infection. PLoS Pathog. 2013; 9:e1003171. [PubMed: 23459099]

Cocchiaro JL, Kumar Y, Fischer ER, Hackstadt T, Valdivia RH. Cytoplasmic lipid droplets are translocated into the lumen of the *Chlamydia trachomatis* parasitophorous vacuole. Proc Natl Acad Sci U S A. 2008; 105:9379–9384. [PubMed: 18591669]

Cortes C, Rzomp KA, Tvinnereim A, Scidmore MA, Wizel B. *Chlamydia pneumoniae* inclusion membrane protein Cpn0585 interacts with multiple Rab GTPases. Infect Immun. 2007; 75:5586–5596. [PubMed: 17908815]

Dumoux M, Clare DK, Saibil HR, Hayward RD. Chlamydiae assemble a pathogen synapse to hijack the host endoplasmic reticulum. Traffic. 2012; 13:1612–1627. [PubMed: 22901061]

Dunning Hotopp JC, Lin M, Madupu R, Crabtree J, Angiuoli SV, Eisen JA, et al. Comparative genomics of emerging human ehrlichiosis agents. PLoS Genet. 2006; 2:e21. [PubMed: 16482227]

Ge Y, Rikihisa Y. Identification of novel surface proteins of *Anaplasma phagocytophilum* by affinity purification and proteomics. J Bacteriol. 2007; 189:7819–7828. [PubMed: 17766422]

Gold DA, Kaplan AD, Lis A, Bett GC, Rosowski EE, Cirelli KM, et al. The *Toxoplasma* dense granule proteins GRA17 and GRA23 mediate the movement of small molecules between the host and the parasitophorous vacuole. Cell Host Microbe. 2015; 17:642–652. [PubMed: 25974303]

Hackstadt T, Scidmore MA, Rockey DD. Lipid metabolism in *Chlamydia trachomatis*-infected cells: directed trafficking of Golgi-derived sphingolipids to the chlamydial inclusion. Proc Natl Acad Sci U S A. 1995; 92:4877–4881. [PubMed: 7761416]

Hackstadt T, Rockey DD, Heinzen RA, Scidmore MA. *Chlamydia trachomatis* interrupts an exocytic pathway to acquire endogenously synthesized sphingomyelin in transit from the Golgi apparatus to the plasma membrane. EMBO J. 1996; 15:964–977. [PubMed: 8605892]

Henderson B, Martin A. Bacterial virulence in the moonlight: multitasking bacterial moonlighting proteins are virulence determinants in infectious disease. Infect Immun. 2011; 79:3476–3491. [PubMed: 21646455]

Henderson B, Martin A. Bacterial moonlighting proteins and bacterial virulence. Curr Top Microbiol Immunol. 2013; 358:155–213. [PubMed: 22143554]

Heuer D, Rejman Lipinski A, Machuy N, Karlas A, Wehrens A, Siedler F, et al. Chlamydia causes fragmentation of the Golgi compartment to ensure reproduction. Nature. 2009; 457:731–735. [PubMed: 19060882]

Huang B, Hubber A, McDonough JA, Roy CR, Scidmore MA, Carlyon JA. The *Anaplasma phagocytophilum*-occupied vacuole selectively recruits Rab-GTPases that are predominantly associated with recycling endosomes. Cell Microbiol. 2010a; 12:1292–1307. [PubMed: 20345488]

Huang B, Troese MJ, Howe D, Ye S, Sims JT, Heinzen RA, et al. *Anaplasma phagocytophilum* APH_0032 is expressed late during infection and localizes to the pathogen-occupied vacuolar membrane. Microb Pathog. 2010b; 49:273–284. [PubMed: 20600793]

Huang B, Troese MJ, Ye S, Sims JT, Galloway NL, Borjesson DL, Carlyon JA. *Anaplasma phagocytophilum* APH_1387 is expressed throughout bacterial intracellular development and localizes to the pathogen-occupied vacuolar membrane. Infect Immun. 2010c; 78:1864–1873. [PubMed: 20212090]

IJdo JW, Wu C, Magnarelli LA, Fikrig E. Serodiagnosis of human granulocytic ehrlichiosis by a recombinant HGE-44-based enzyme-linked immunosorbent assay. J Clin Microbiol. 1999; 37:3540–3544. [PubMed: 10523549]

Junutula JR, De Maziere AM, Peden AA, Ervin KE, Advani RJ, van Dijk SM, et al. Rab14 is involved in membrane trafficking between the Golgi complex and endosomes. Mol Biol Cell. 2004; 15:2218–2229. [PubMed: 15004230]

Kahlon A, Ojogun N, Ragland SA, Seidman D, Troese MJ, Ottens AK, et al. *Anaplasma phagocytophilum* Asp14 is an invasin that interacts with mammalian host cells via its C terminus to facilitate infection. Infect Immun. 2013; 81:65–79. [PubMed: 23071137]

Kholti A, Charlier D, Gigot D, Huysveld N, Roovers M, Glansdorff N. pyrH-encoded UMP-kinase directly participates in pyrimidine-specific modulation of promoter activity in *Escherichia coli*. J Mol Biol. 1998; 280:571–582. [PubMed: 9677289]

Klein MB, Miller JS, Nelson CM, Goodman JL. Primary bone marrow progenitors of both granulocytic and monocytic lineages are susceptible to infection with the agent of human granulocytic ehrlichiosis. J Infect Dis. 1997; 176:1405–1409. [PubMed: 9359749]

Landais S, Gounon P, Laurent-Winter C, Mazie JC, Danchin A, Barzu O, Sakamoto H. Immunochemical analysis of UMP kinase from *Escherichia coli*. J Bacteriol. 1999; 181:833–840. [PubMed: 9922246]

Lev S. Non-vesicular lipid transport by lipid-transfer proteins and beyond. Nat Rev Mol Cell Biol. 2010; 11:739–750. [PubMed: 20823909]

Lin M, Rikihisa Y. *Ehrlichia chaffeensis* and *Anaplasma phagocytophilum* lack genes for lipid A biosynthesis and incorporate cholesterol for their survival. Infect Immun. 2003; 71:5324–5331. [PubMed: 12933880]

Lipinski AR, Heymann J, Meissner C, Karlas A, Brinkmann V, Meyer TF, Heuer D. Rab6 and Rab11 regulate *Chlamydia trachomatis* development and Golgin-84-dependent Golgi fragmentation. PLoS Pathog. 2009; 5:e1000615. [PubMed: 19816566]

Liu S, Storrie B. Are Rab proteins the link between Golgi organization and membrane trafficking? Cell Mol Life Sci. 2012; 69:4093–4106. [PubMed: 22581368]

Mastronunzio JE, Kurscheid S, Fikrig E. Postgenomic analyses reveal development of infectious *Anaplasma phagocytophilum* during transmission from ticks to mice. J Bacteriol. 2012; 194:2238–2247. [PubMed: 22389475]

van Meer G. Lipids of the Golgi membrane. Trends Cell Biol. 1998; 8:29–33. [PubMed: 9695805]

Mishra MK, Gerard HC, Whittum-Hudson JA, Hudson AP, Kannan RM. Dendrimer-enabled modulation of gene expression in *Chlamydia trachomatis*. Mol Pharm. 2012; 9:413–421. [PubMed: 22263556]

Mott J, Barnewall RE, Rikihisa Y. Human granulocytic ehrlichiosis agent and *Ehrlichia chaffeensis* reside in different cytoplasmic compartments in HL-60 cells. Infect Immun. 1999; 67:1368–1378. [PubMed: 10024584]

Munderloh UG, Lynch MJ, Herron MJ, Palmer AT, Kurtti TJ, Nelson RD, Goodman JL. Infection of endothelial cells with *Anaplasma marginale* and *A. phagocytophilum*. Vet Microbiol. 2004; 101:53–64. [PubMed: 15201033]

Niu H, Xiong Q, Yamamoto A, Hayashi-Nishino M, Rikihisa Y. Autophagosomes induced by a bacterial Beclin 1 binding protein facilitate obligatory intracellular infection. Proc Natl Acad Sci U S A. 2012; 109:20800–20807. [PubMed: 23197835]

Ojogun N, Kahlon A, Ragland SA, Troese MJ, Mastronunzio JE, Walker NJ, et al. *Anaplasma phagocytophilum* outer membrane protein A interacts with sialylated glycoproteins to promote infection of mammalian host cells. Infect Immun. 2012; 80:3748–3760. [PubMed: 22907813]

Pagano RE, Martin OC, Kang HC, Haugland RP. A novel fluorescent ceramide analogue for studying membrane traffic in animal cells: accumulation at the Golgi apparatus results in altered spectral properties of the sphingolipid precursor. J Cell Biol. 1991; 113:1267–1279. [PubMed: 2045412]

Rzomp KA, Scholtes LD, Briggs BJ, Whittaker GR, Scidmore MA. Rab GTPases are recruited to chlamydial inclusions in both a species-dependent and species-independent manner. Infect Immun. 2003; 71:5855–5870. [PubMed: 14500507]

Scidmore MA, Fischer ER, Hackstadt T. Sphingolipids and glycoproteins are differentially trafficked to the *Chlamydia trachomatis* inclusion. J Cell Biol. 1996; 134:363–374. [PubMed: 8707822]

Seidman D, Ojogun N, Walker NJ, Mastronunzio J, Kahlon A, Hebert KS, et al. *Anaplasma phagocytophilum* surface protein AipA mediates invasion of mammalian host cells. Cell Microbiol. 2014; 16:1133–1145. [PubMed: 24612118]

Sherwood RK, Roy CR. A Rab-centric perspective of bacterial pathogen-occupied vacuoles. Cell Host Microbe. 2013; 14:256–268. [PubMed: 24034612]

Simanshu DK, Kamlekar RK, Wijesinghe DS, Zou X, Zhai X, Mishra SK, et al. Non-vesicular trafficking by a ceramide-1-phosphate transfer protein regulates eicosanoids. Nature. 2013; 500:463–467. [PubMed: 23863933]

Stenmark H. Rab GTPases as coordinators of vesicle traffic. Nat Rev Mol Cell Biol. 2009; 10:513–525. [PubMed: 19603039]

Sukumaran B, Mastronunzio JE, Narasimhan S, Fankhauser S, Uchil PD, Levy R, et al. *Anaplasma phagocytophilum* AptA modulates Erk1/2 signalling. Cell Microbiol. 2011; 13:47–61. [PubMed: 20716207]

Troese MJ, Carlyon JA. *Anaplasma phagocytophilum* dense-cored organisms mediate cellular adherence through recognition of human P-selectin glycoprotein ligand 1. Infect Immun. 2009; 77:4018–4027. [PubMed: 19596771]

Troese MJ, Kahlon A, Ragland SA, Ottens AK, Ojogun N, Nelson KT, et al. Proteomic analysis of *Anaplasma phagocytophilum* during infection of human myeloid cells identifies a protein that is pronouncedly upregulated on the infectious dense-cored cell. Infect Immun. 2011; 79:4696–4707. [PubMed: 21844238]

Truchan HK, Seidman D, Carlyon JA. Breaking in and grabbing a meal: *Anaplasma phagocytophilum* cellular invasion, nutrient acquisition, and promising tools for their study. Microbes and Infection/ Institut Pasteur. 2013; 15:1017–1025. [PubMed: 24141091]

Vromman F, Subtil A. Exploitation of host lipids by bacteria. Curr Opin Microbiol. 2014; 17:38–45. [PubMed: 24581691]

Walker NJ, Clark EA, Ford DC, Bullifent HL, McAlister EV, Duffield ML, et al. Structure and function of cytidine monophosphate kinase from *Yersinia pseudotuberculosis*, essential for virulence but not for survival. Open Biol. 2012; 2:120142. [PubMed: 23271832]

Wang Y, Berg EA, Feng X, Shen L, Smith T, Costello CE, Zhang YX. Identification of surface-exposed components of MOMP of *Chlamydia trachomatis* serovar F. Protein Sci. 2006; 15:122–134. [PubMed: 16322562]

Wijesinghe DS, Brentnall M, Mietla JA, Hoeferlin LA, Diegelmann RF, Boise LH, Chalfant CE. Ceramide kinase is required for a normal eicosanoid response and the subsequent orderly migration of fibroblasts. J Lipid Res. 2014; 55:1298–1309. [PubMed: 24823941]

Wolf K, Hackstadt T. Sphingomyelin trafficking in *Chlamydia pneumoniae*-infected cells. Cell Microbiol. 2001; 3:145–152. [PubMed: 11260137]

Wood DO, Wood RR, Tucker AM. Genetic systems for studying obligate intracellular pathogens: an update. Curr Opin Microbiol. 2014; 17:11–16. [PubMed: 24581687]

Xiong Q, Rikihisa Y. Subversion of NPC1 pathway of cholesterol transport by *Anaplasma phagocytophilum*. Cell Microbiol. 2012; 14:560–576. [PubMed: 22212234]

Xiong Q, Lin M, Rikihisa Y. Cholesterol-dependent *Anaplasma phagocytophilum* exploits the low-density lipoprotein uptake pathway. PLoS Pathog. 2009; 5:e1000329. [PubMed: 19283084]

Yan H, Tsai MD. Nucleoside monophosphate kinases: structure, mechanism, and substrate specificity. Adv Enzymol Relat Areas Mol Biol. 1999; 73:103–134. [PubMed: 10218107]

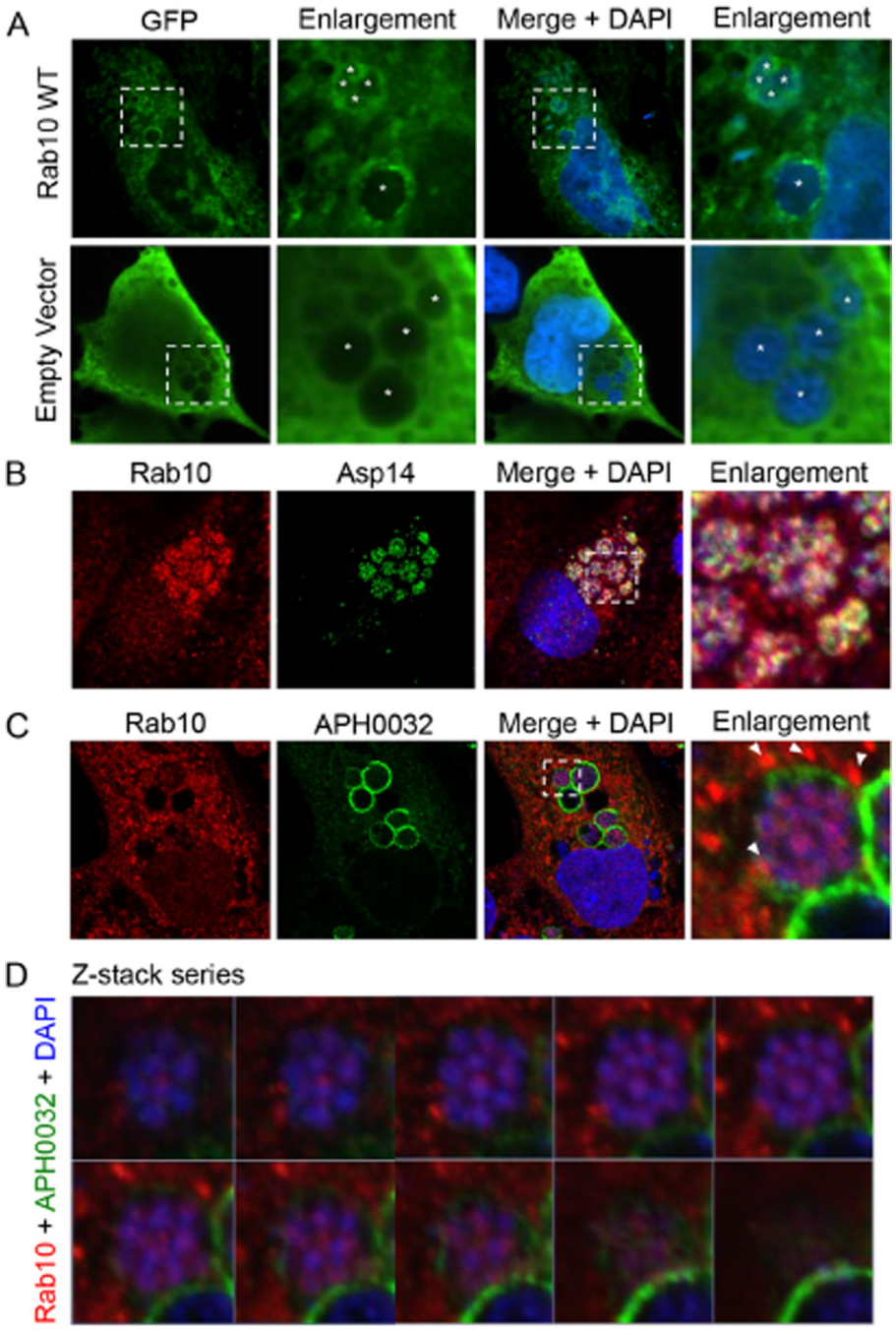

Fig. 1.

Endogenous and ectopically expressed Rab10 localize to the AVM and with intravacuolar *A. phagocytophilum* organisms.

A. GFP-Rab10 localizes to the AVM and with intravacuolar bacteria. RF/6A cells expressing GFP-Rab10 were infected with *A. phagocytophilum* and visualized by LSCM. Asterisks denote bacterial vacuoles.

B. Endogenous Rab10 localizes with *A. phagocytophilum* surface protein Asp14. *A. phagocytophilum*-infected RF/6A cells that had been screened with antibodies against Rab10 and Asp14 were examined by confocal microscopy.

C, D. Z-stack series and 3D rendering show endogenous Rab10 associated with *A. phagocytophilum* organisms within the ApV. *A. phagocytophilum*-infected RF/6A cells were screened with antibodies against Rab10 and AVM protein APH0032 and visualized by confocal microscopy. (C) Representative infected host cell that was used for Z-stack analysis. Note the localization of punctate Rab10 labelling at the AVM (arrow heads) and within the ApV associated with *A. phagocytophilum* organisms. (D) Z-stack series showing individual, successive focal planes. (A–C) The regions in the merge + DAPI panels that are demarcated by hatched-line boxes indicate the regions that are magnified in the enlargement panels. The enlargement panel in C was analysed by Z-stack in (D) (A–D) Host cell nuclei and bacterial DNA were stained with DAPI (blue). Results shown are representative of three experiments with similar results.

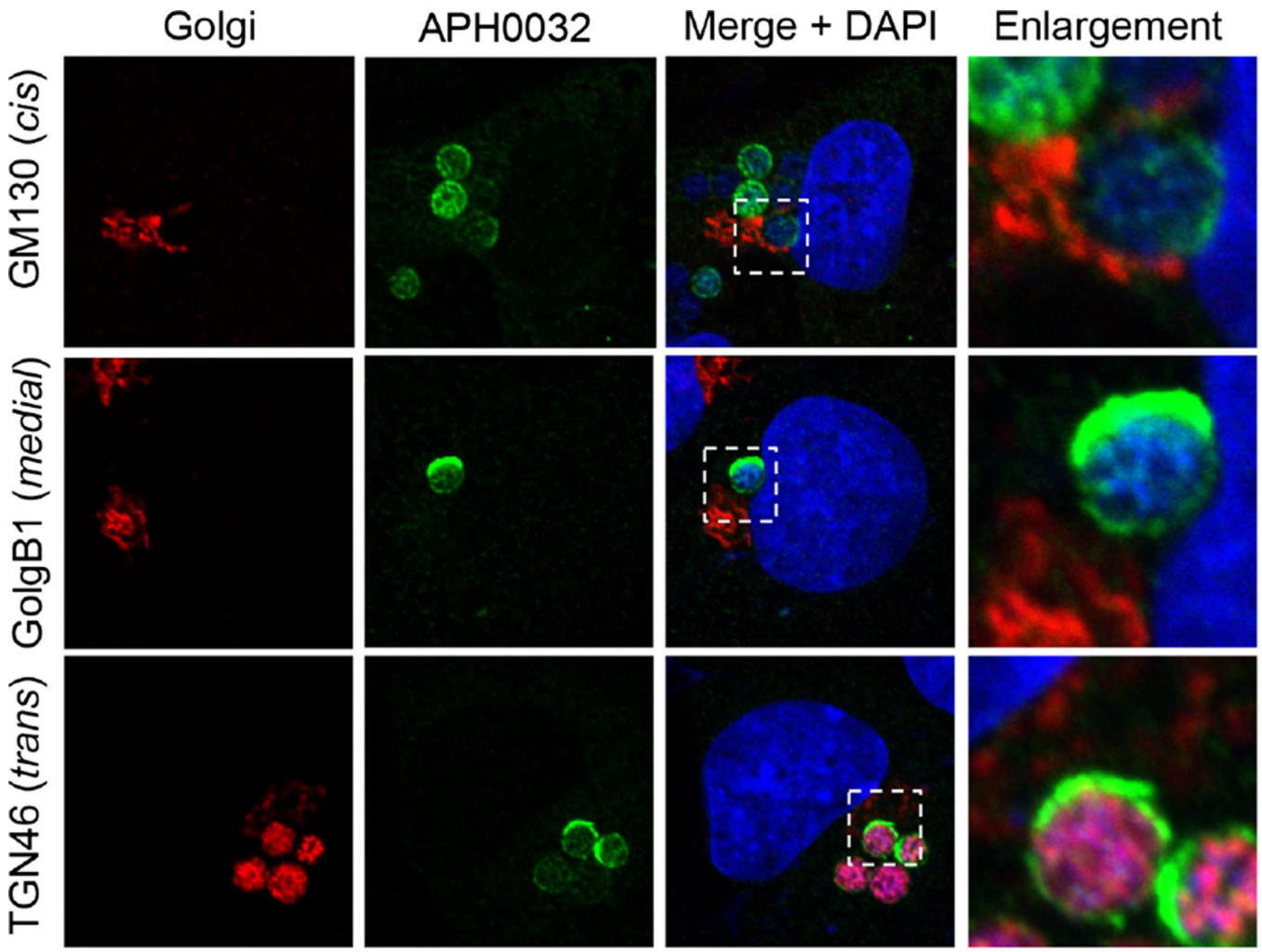

Fig. 2.

The ApV localizes adjacent to the Golgi apparatus, and TGN-derived vesicles are delivered into its lumen. *Anaplasma phagocytophilum* infected RF/6A cells were screened with antibodies against AVM marker, APH0032, and GM130 (*cis*-Golgi), GolgB1 (*cis*-Golgi and *medial*-Golgi) or TGN46 (*trans*-Golgi) and examined using LSCM. Results shown are representative of three experiments with similar results.

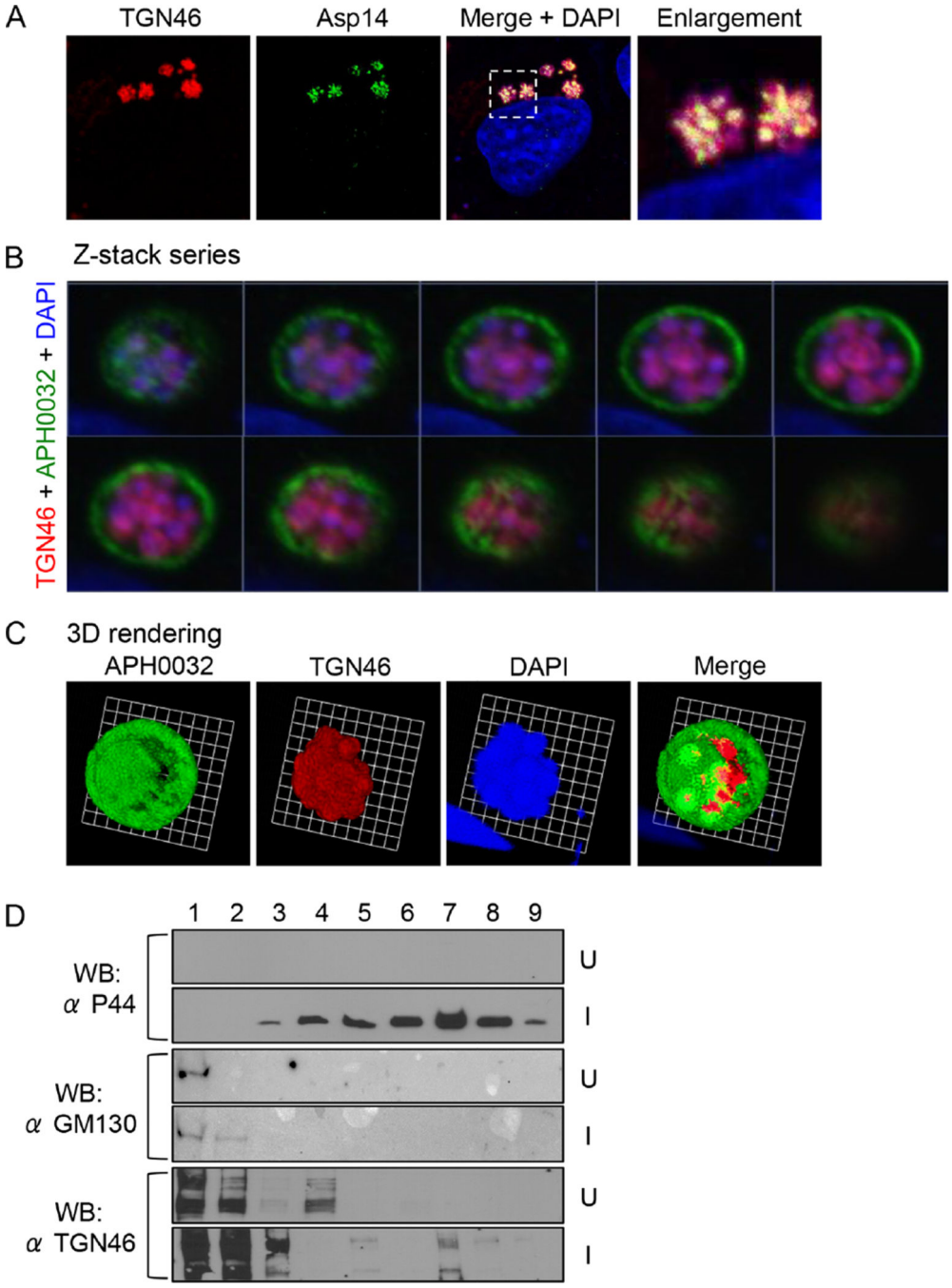

Fig. 3.

The ApV localizes adjacent to the Golgi apparatus, and TGN-derived vesicles are delivered into the ApV lumen where they associate with *A. phagocytophilum* organisms.

A. TGN46 signal colocalizes with intravacuolar bacteria. *A. phagocytophilum*-infected cells were screened with antibodies against TGN46 and Asp14 and examined by LSCM. The region that is demarcated by a hatched-line box is magnified in the enlargement panel.

B. Z-stack series shows TGN46 within the ApV. *A. phagocytophilum*-infected RF/6A cells were screened with antibodies against TGN46 and APH0032. Successive focal planes of a representative *A. phagocytophilum* vacuole are presented.

C. 3D rendering of the Z-stack series presented in B shows TGN46-positive vesicles encasing individual *A. phagocytophilum* organisms within the vacuole. These 3D images are also presented in Movie S2.

D. TGN46 cofractionates with *A. phagocytophilum* organisms. Uninfected (U) or *A. phagocytophilum*-infected HL-60 cells (I) were homogenized, and the post-nuclear supernatants were subjected to density gradient centrifugation. Successive 1 ml aliquots were analysed by Western blot (WB) using antibodies against TGN46, GM130 and *A. phagocytophilum* major surface protein, P44. Results shown are representative of three experiments with similar results.

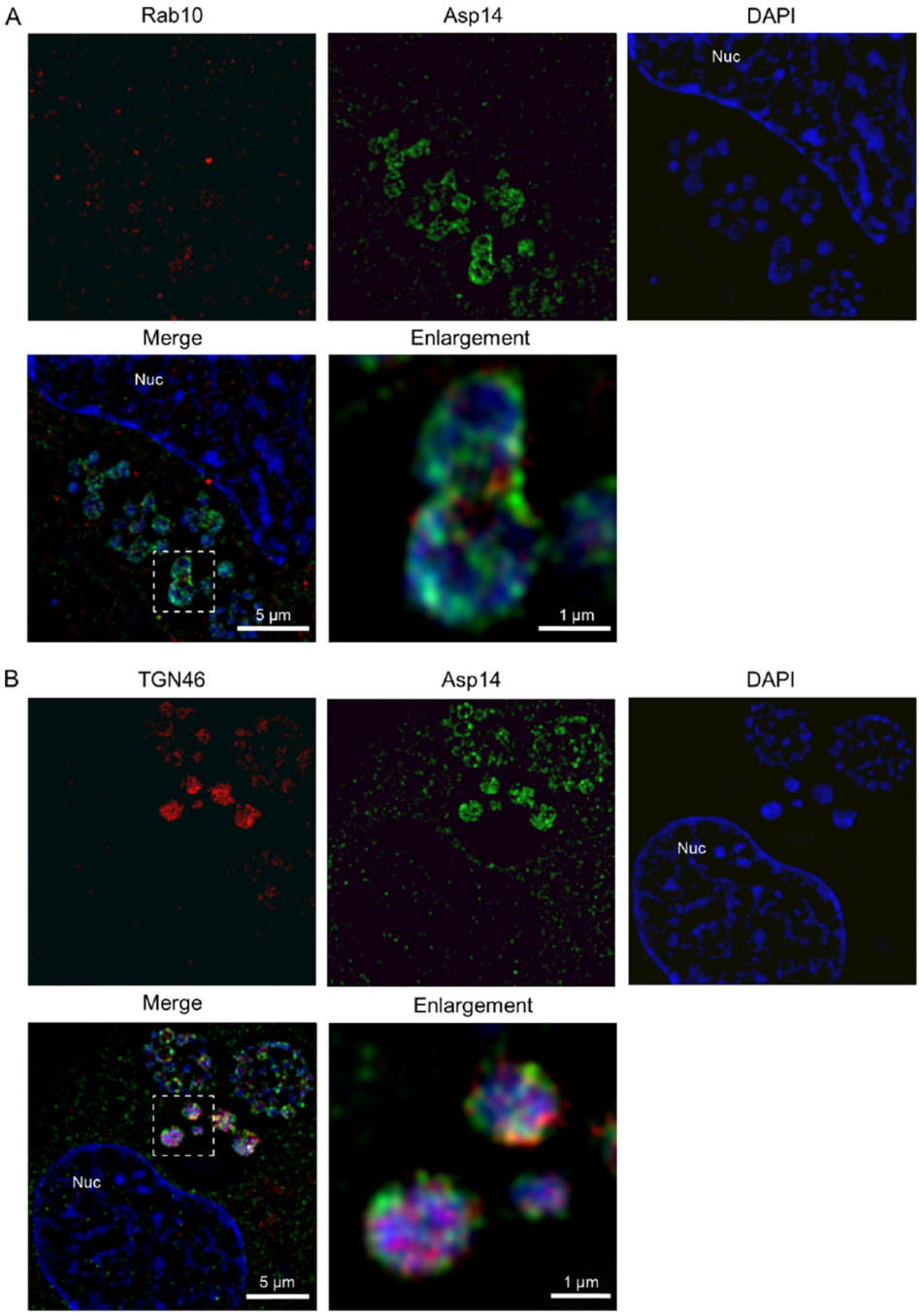

Fig. 4.

Structured illumination microscopic analyses confirm that Rab10-positive and TGN46-positive vesicles are present in the ApV proximally associated with intravacuolar *A. phagocytophilum* organisms.

A, B. *A. phagocytophilum*-infected RF/6A cells that had been screened with antibodies against (A) Rab10 and Asp14 or (B) TGN46 and Asp14 were examined by SIM. The regions in the merge + DAPI panels that are demarcated by hatched-line boxes indicate the regions that are magnified in the enlargement panels. Host cell nuclei and bacterial DNA

were stained with DAPI (blue). Results shown are representative of three experiments with similar results. Nuc, host cell nucleus.

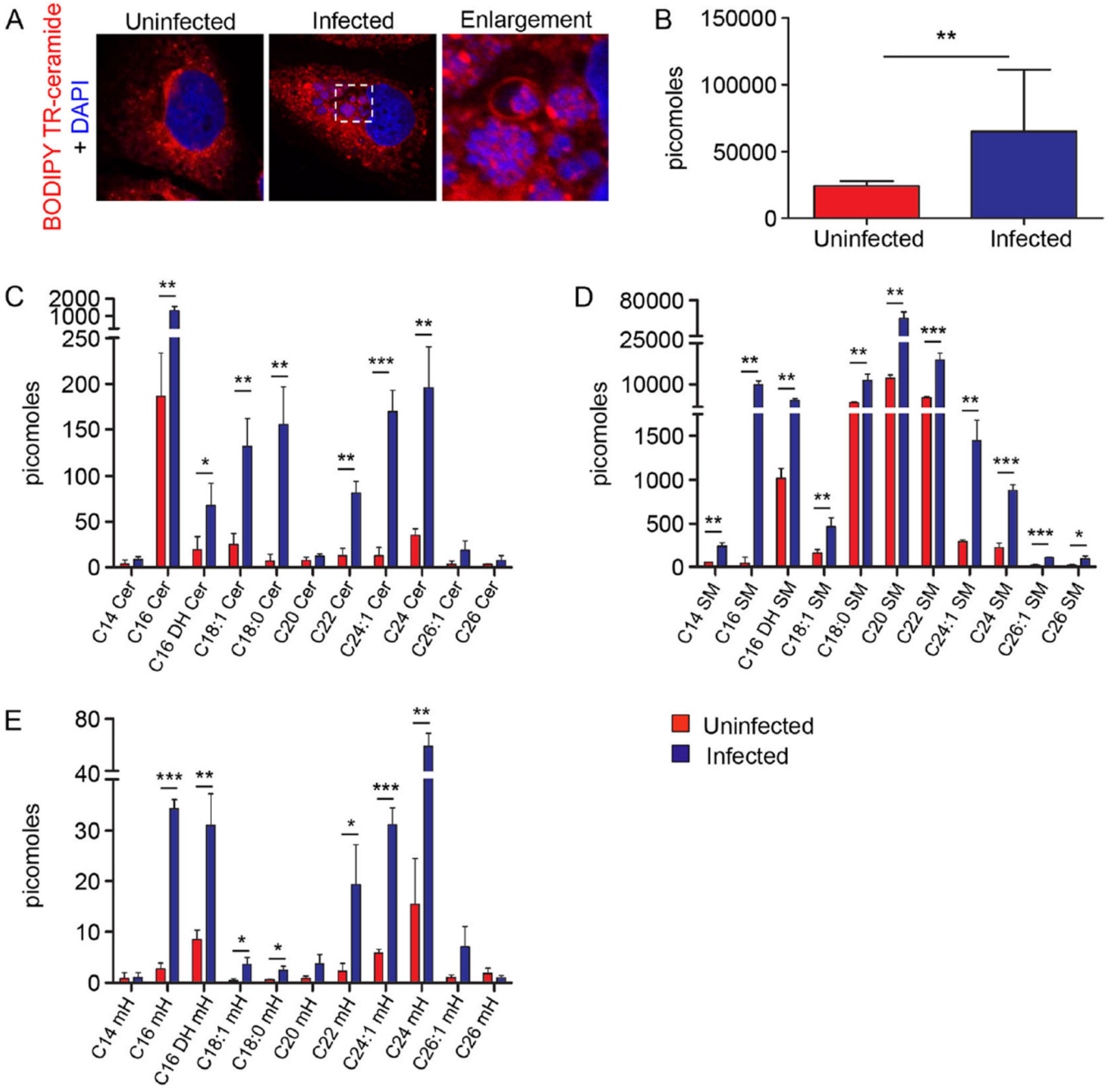

Fig. 5.

Sphingolipids are delivered into the ApV and incorporated by *A. phagocytophilum*.

A. BODIPY TR-labelled sphingolipids localize with intravacuolar *A. phagocytophilum* organisms. BODIPY TR ceramide was added to uninfected and *A. phagocytophilum*-infected cells and examined by LSCM. Host cell nuclei and bacterial DNA were stained with DAPI (blue). Results are representative of three experiments.

B–E. *A. phagocytophilum* incorporates host cell sphingolipids. Host cell-free *A. phagocytophilum* DC organisms recovered from the media of infected HL-60 cells were subjected to UPLC-ESI-MS/MS to detect total sphingolipids (B), ceramides (Cer) (C),

sphingomyelins (SM) (D) and monohexosyl sphingolipids (mH) (E). Media from uninfected HL-60 cells was processed and examined in parallel. Results are the mean ± standard deviation of triplicate samples and are representative of three biological replicates with similar results. Statistically significant (*$P \leq 0.05$; **$P \leq 0.01$; ***$P \leq 0.001$) values are indicated.

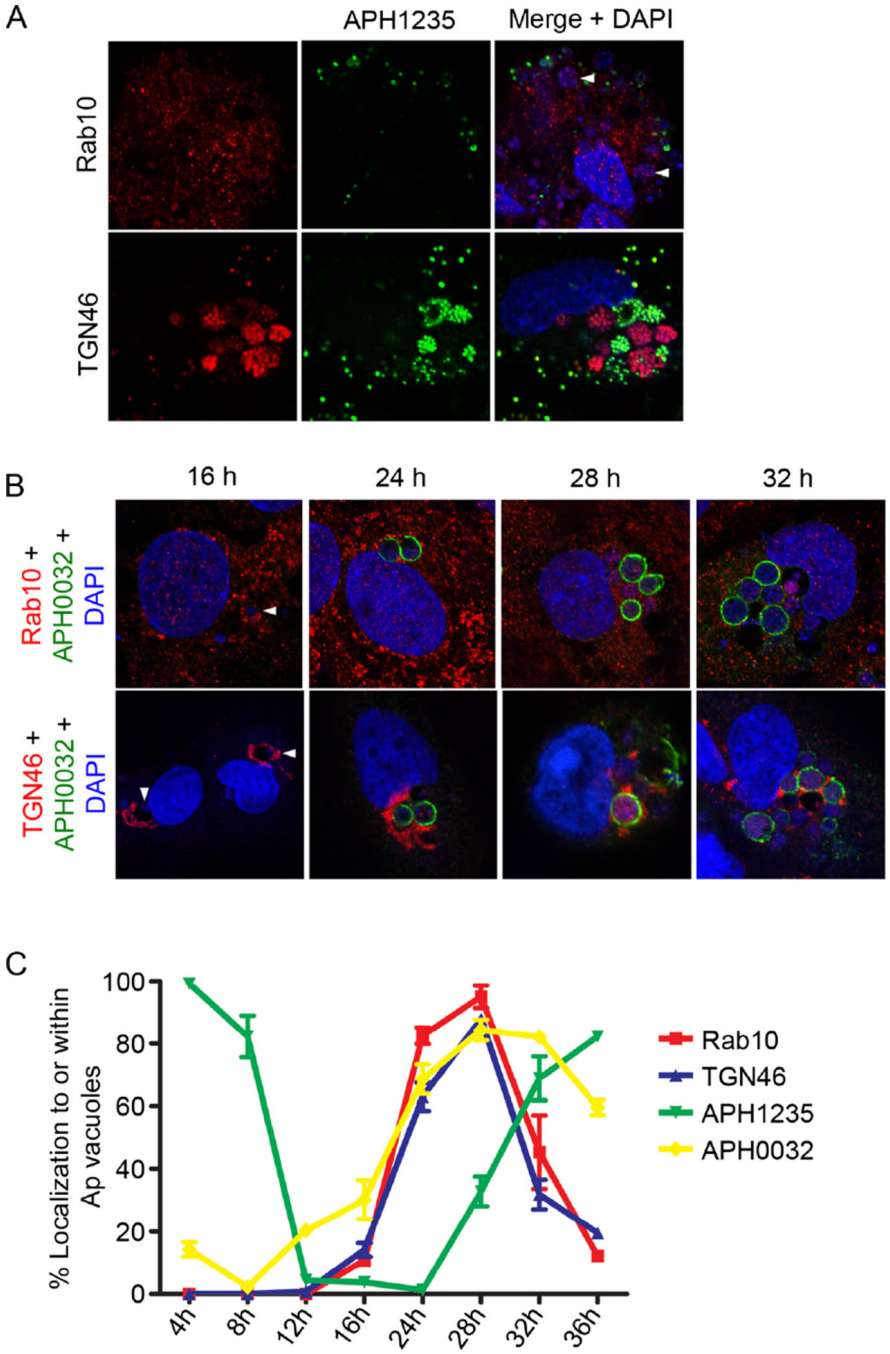

Fig. 6.

A. phagocytophilum acquisition of Rab10-positive TGN vesicles precedes conversion to the APH1235-positive infectious DC form.

A. Rab10 and TGN46 colocalize with *A. phagocytophilum* organisms during the replicative phase of bacterial development. *A. phagocytophilum* infected RF/6A cells were screened with antibodies against Rab10 or TGN46 and the *A. phagocytophilum* DC marker, APH1235.

B, C. RF/6A cells were synchronously infected with *A. phagocytophilum*, stained with DAPI, screened with antibodies against *A. phagocytophilum* Rab10, TGN46, APH1235 and APH0032 and examined by confocal microscopy at 4, 8, 12, 16, 24, 28 and 32 h post-infection. Results shown are representative of three experiments. (B) Representative confocal micrograph images of *A. phagocytophilum*-infected cells at 16, 24, 28 and 32 h screened with APH0032 and either Rab10 or TGN46 antibodies. Data are representative of three experiments with similar results.

A and B. Arrowheads denote ApVs in (A) and (B) because the antibody against the AVM marker, APH0032, was not used in (A) and *A. phagocytophilum* does not abundantly express APH0032 at 16 h. (C) Acquisition of TGN46 and Rab10 by *A. phagocytophilum* precedes bacterial expression of APH1235. Percentages of ApVs that were positive for Rab10, TGN46, APH135 and APH0032 over the time course are presented. Data are the mean (± standard deviation) of triplicate samples and are representative of two experiments with similar results.

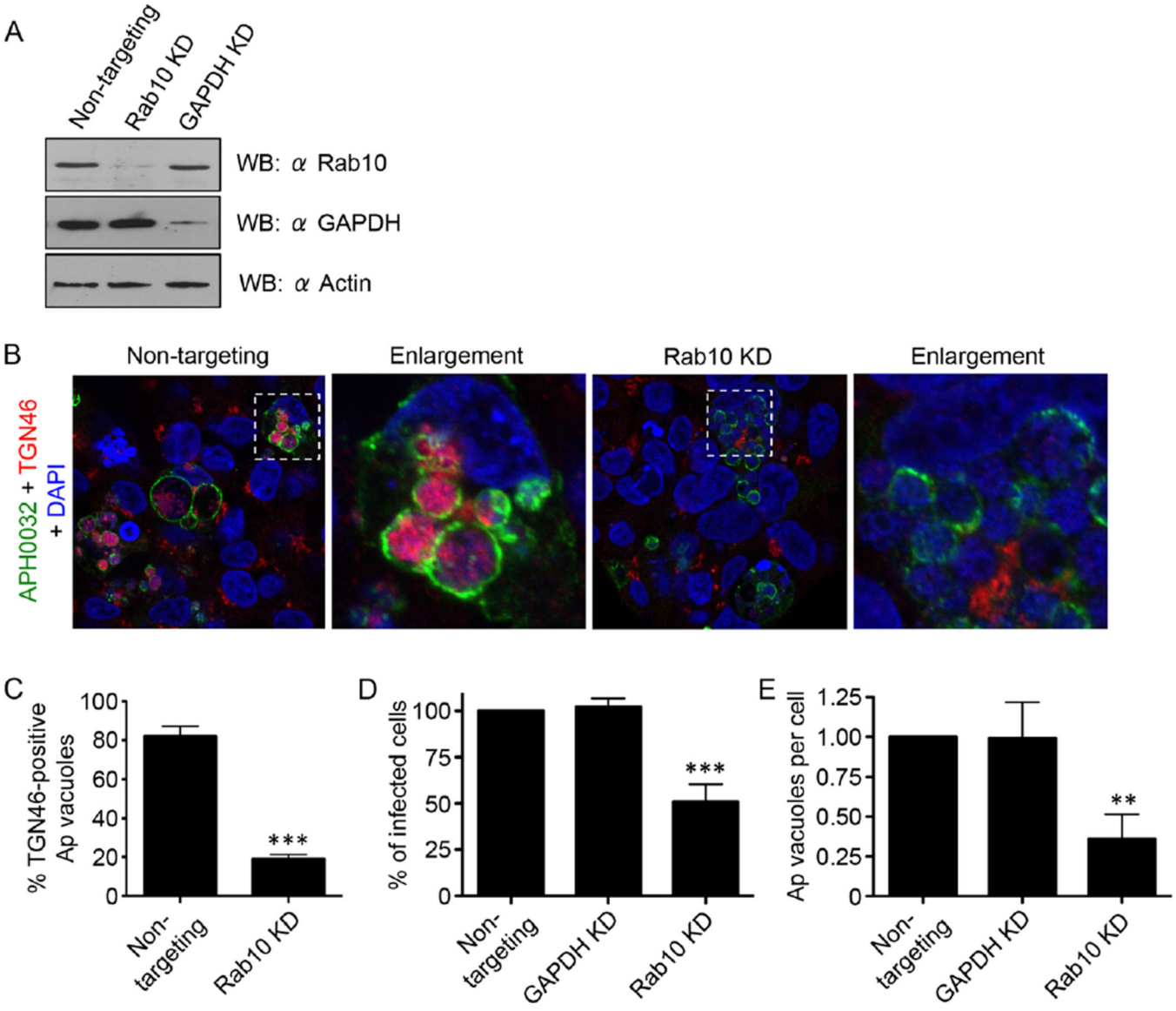

Fig. 7.

Knockdown of Rab10 markedly reduces both TGN vesicle delivery into the ApV and *A. phagocytophilum* infection. HEK-293T cells were treated with Rab10-targeting, non-targeting or GAPDH-targeting siRNA for 72 h.

A. Western blot showing knockdown of Rab10 or GAPDH after appropriate siRNA treatment.

B–D. After siRNA treatment, the cells were infected with *A. phagocytophilum* (Ap) for 48 h and processed for confocal microscopy. (B and C) Rab10 knockdown markedly inhibits translocation of TGN vesicles into the ApV. Rab10-targeting and non-targeting siRNA-treated infected cells were screened with antibodies against APH0032 and TGN46 and stained with DAPI (blue). (B) Representative confocal micrographs. Regions that are demarcated by hatched-line boxes are magnified in the corresponding enlargement panels. (C) Percentage ± standard deviation (SD) of TGN46-positive ApVs in non-targeting siRNA-

treated or Rab10-targeting siRNA-treated infected cells. (D and E) Rab10 knockdown (KD) significantly reduces *A. phagocytophilum* infection. siRNA-treated infected cells were screened with an antibody against *A. phagocytophilum* P44 to denote bacteria and examined by immunofluorescence microscopy to determine the percentage ± SD of infected cells (D) and mean number ± SD of ApVs per cell (E). Statistically significant (** $P \leq 0.01$; *** $P \leq 0.001$) values are indicated. Data presented in each panel are representative of three experiments with similar results.

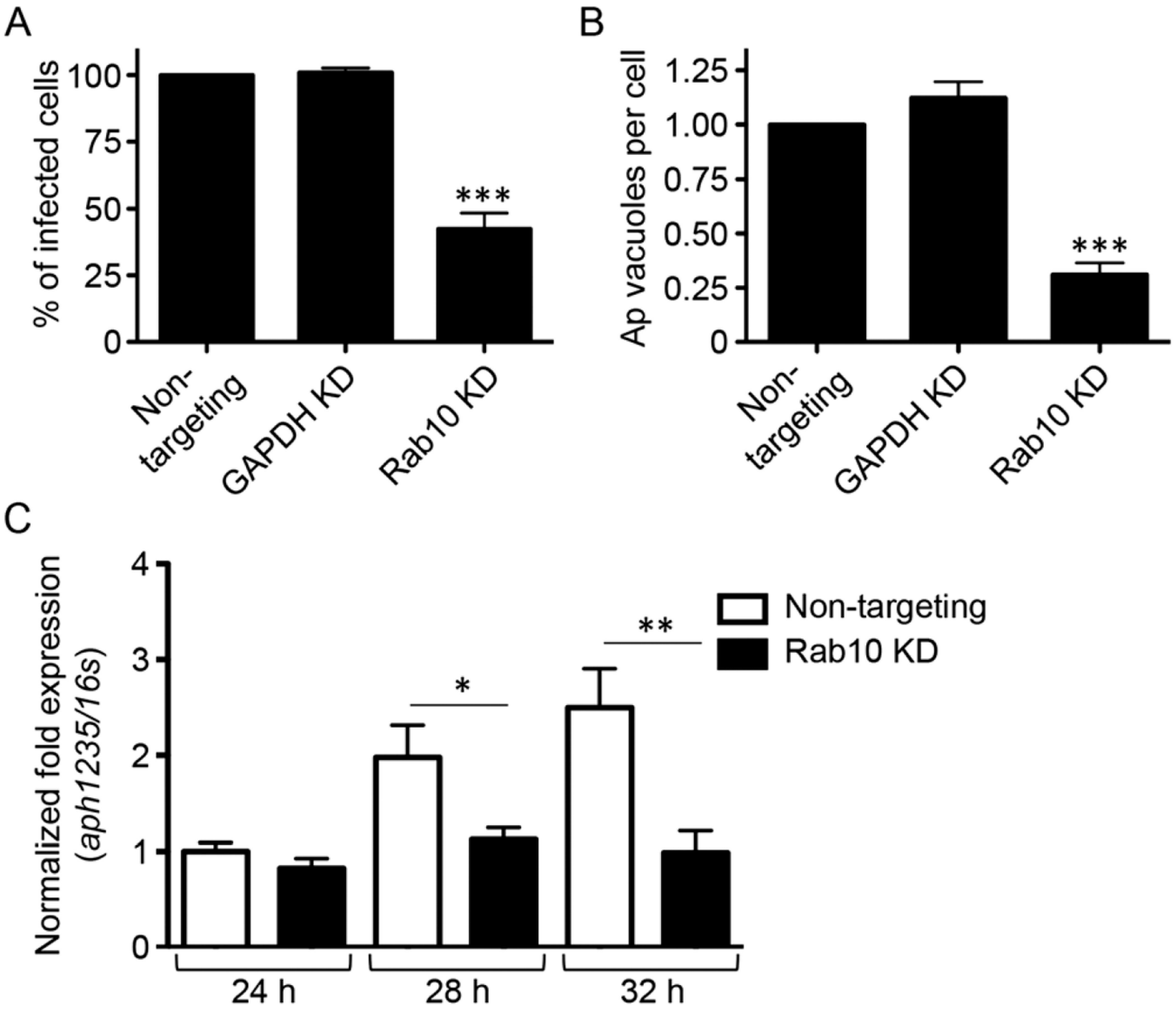

Fig. 8.

Knockdown of Rab10 markedly reduces generation of infectious progeny and *aph1235* transcription.

A. Rab10 knockdown (KD) reduces generation of infectious progeny. HEK-293T cells were treated with Rab10-targeting, GAPDH-targeting or non-targeting siRNA for 72 h and subsequently infected with *A. phagocytophilum* (Ap). At 48 h post-infection, a time point at which infectious DC organisms would be present in the media if the bacterial developmental cycle had proceeded normally, media from the infected siRNA-treated cells was added to naïve HEK-293T cells. At 24 h, the recipient cells were screened with antibody against Ap P44 and examined by immunofluorescence microscopy to determine the percentages of infected cells (A) and the mean number (± standard deviation) of ApVs per cell (B). Data presented are representative of three experiments with similar results.

C. Knocking down Rab10 inhibits transcription of the Ap DC marker, *aph1235*. Total RNAs isolated from non-targeting siRNA-treated or Rab10-targeting siRNA-treated, Ap-infected cells at 24, 28 and 32 h were subjected to qRT-PCR using primers specific for *aph1235*. Relative *aph1235* transcript levels were normalized to Ap 16S rRNA gene transcript levels using the $2^{-\Delta\Delta CT}$ method. Data presented are representative of two experiments with similar results. Statistically significant (*$P \leq 0.05$; **$P \leq 0.01$; ***$P \leq 0.001$) values are indicated.

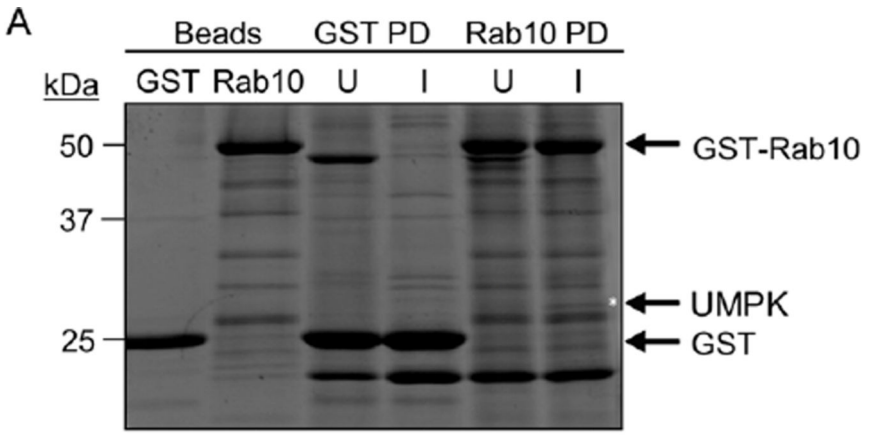

B

MSIDCNVVENVRYSRVLLKVSGEALAGERGFGFDQDVIGKLSCDLKKVRESGVELCIV
VGGGNIFRGSSTSFGFERASNDYVGMLATMINALALQNSLEDMGIASRVLSAIPMTAV
CETYIRRRAIRHLEKGRVVICAAGIGSPFFTTDTAAVLRSIEMRCDAIFKGTQVDGVYSS
DPKKDCSATRYDKISYHDLLASDLKIMDAAAVSLARENSIPIIVFDLGKENAFSEVMKGR
GTFTTISG

Fig. 9.

Identification of an *A. phagocytophilum* Rab10-specific ligand.

A. GST-Rab10 beads pull down *A. phagocytophilum* UMPK (APH0111). Glutathione sepharose beads coupled with GST-Rab10 or GST alone were incubated with whole-cell lysates of uninfected or *A. phagocytophilum*-infected HL-60 cells. Eluates from pulldown beads and beads alone were resolved by SDS-PAGE and stained with Sypro Ruby. The band of approximately 26 kDa (denoted by asterisk) that was unique to the eluate from GST-Rab10 beads incubated with *A. phagocytophilum*-infected cell lysate was excised and analysed by mass spectroscopy. PD, pulldown. U, uninfected. I, infected.

B. *A. phagocytophilum* UMPK amino acid sequence. Underlined peptide sequences are those that were identified by LC-MS/MS following precipitation of UMPK by GST-Rab10. Peptides that were identified as being on the *A. phagocytophilum* surface in our prior report (Kahlon *et al.*, 2013) are denoted by green highlighting. Blue highlighting demarcates predicted transmembrane domains. Red highlighting indicates the peptide encompassing amino acids 182–195 against which antiserum was raised.

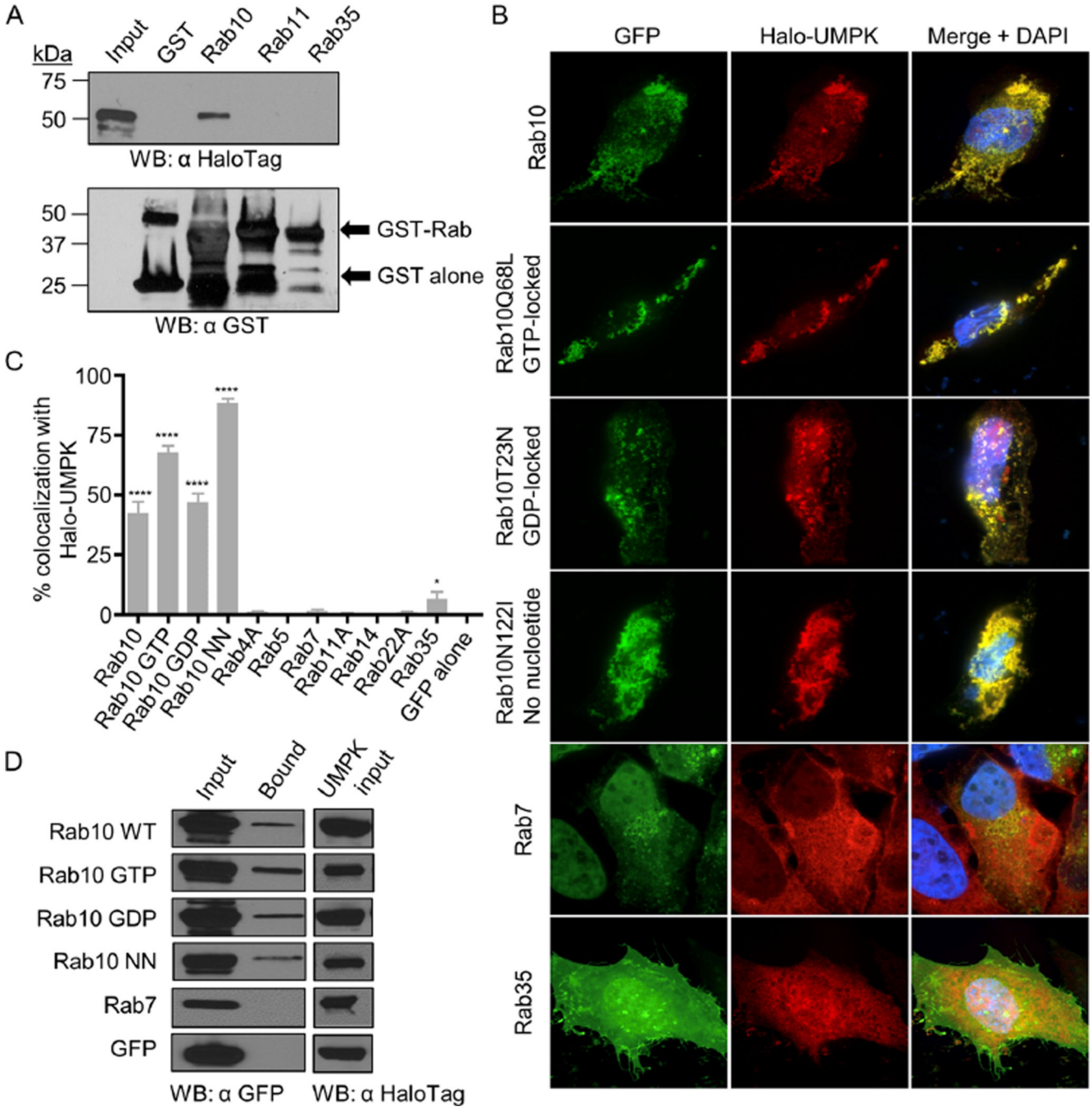

Fig. 10.

Validation of *A. phagocytophilum* UMPK-Rab10 interactions.

A. GST-Rab10 but not other GST-tagged Rabs or GST alone pull down UMPK. A lysate of *E. coli* expressing Halo-UMPK was divided equally and incubated with GST, GST-Rab10, GST-Rab11 and GST-Rab35 coated beads. Input *E. coli* lysate and bead eluates were analysed by immunoblot using HaloTag and GST antibodies.

B. Halo-UMPK colocalizes specifically with vesicles that are positive for GFP-Rab10 isoforms in an aggregative pattern. HeLa cells were cotransfected to express Halo-UMPK

together with GFP-Rab10 isoforms or other GFP-tagged Rab GTPases and analysed by confocal microscopy. Rab10Q68L (GTP locked); Rab10T32N (GDP locked); Rab10N122I [incapable of binding any GTP or GDP (no nucleotide)].

C. Vesicles that are positive for GFP-Rab10 isoforms differentially colocalize with UMPK. One hundred cells coexpressing Halo-tagged *A. phagocytophilum* UMPK and GFP-tagged Rab GTPases or Halo-tagged *E. coli* UMPK and GFP-Rab10 were assessed per condition for Halo and GFP signal colocalization. Statistically significant (**** $P \leq 0.0001$; * $P \leq 0.05$) values are indicated.

D. Halo-UMPK interacts with all Rab10 isoforms in living cells. HeLa cells were cotransfected to express Halo-UMPK together with GFP-Rab10 isoforms, GFP-Rab7 or GFP alone. Whole-cell lysates of the transfected cells (Input) were mixed with Halo-Link resin, and the resin eluate (Bound) was analysed by Western blot (WB) with GFP antibody. Portions of each transfection lysate were analysed with HaloTag antibody to confirm Halo-UMPK bait expression (UMPK input). Data presented in A and D are representative of two experiments with similar results. Data presented in B and C are representative of three experiments with similar results.

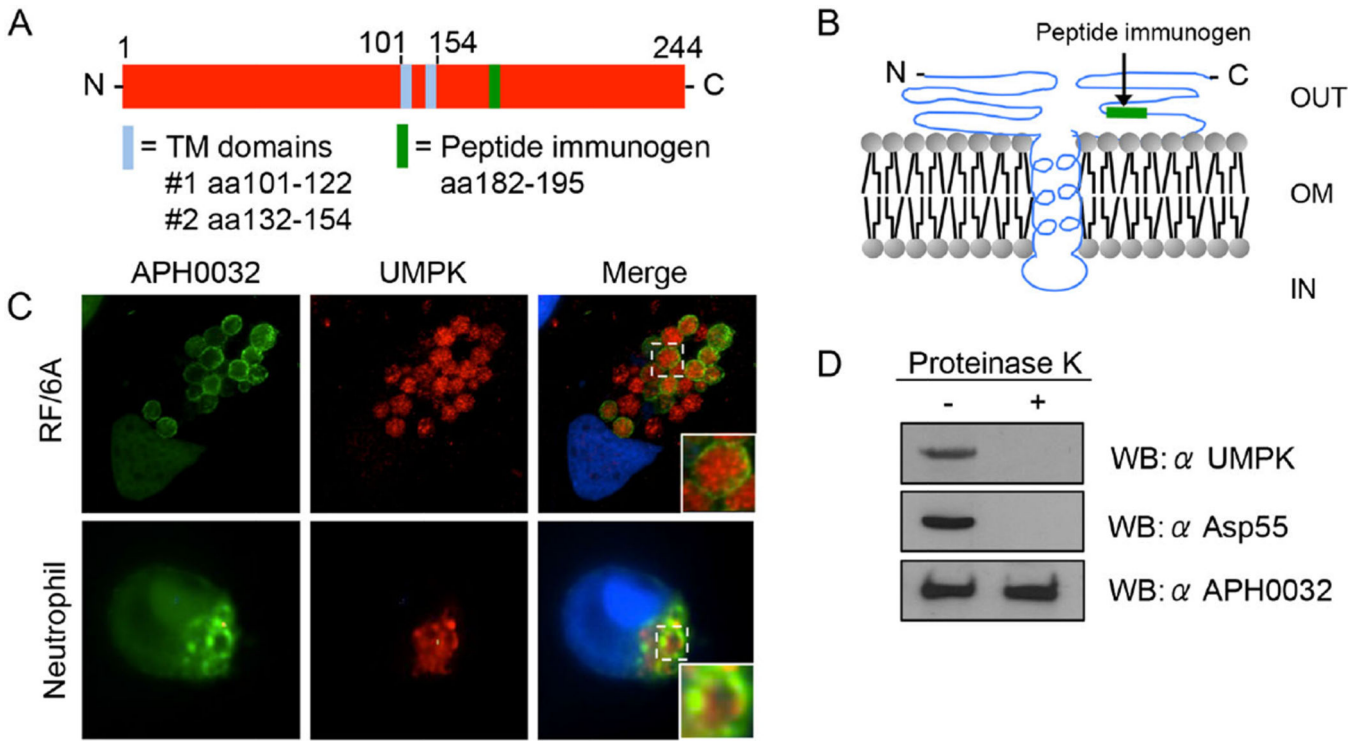

Fig. 11.

UMPK is an *A. phagocytophilum* surface protein.

A. UMPK is a 244-amino-acid protein with two predicted TM domains at residues 101–122 and 132–154. Antiserum was raised against a peptide that corresponds to amino acids 182–195, which is predicted to be surface exposed.

B. Predicted outer membrane (OM) topology of UMPK. OUT, extracellular. IN, interior to the OM.

C. UMPK localizes within the ApV. *A. phagocytophilum*-infected RF/6A cells, and human neutrophils were screened with antibodies against UMPK and APH0032 and visualized by confocal microscopy. The insets denoted by solid boxes are enlarged versions of the vacuoles demarcated by hatched-line boxes. Host cell nuclei and bacterial DNA were stained with DAPI (blue).

D. Proteinase K removes a surface-exposed UMPK epitope. Intact *A. phagocytophilum* organisms were incubated with proteinase K (+) or vehicle control (−) followed by washing to remove cleaved proteins. The bacteria were lysed and analysed by Western blot (WB) using antibodies against UMPK residues 182–195, a known-surface exposed epitope of the *A. phagocytophilum* surface protein, Asp55, and APH0032, which is not a surface protein. Results presented are representative of two experiments with similar results.

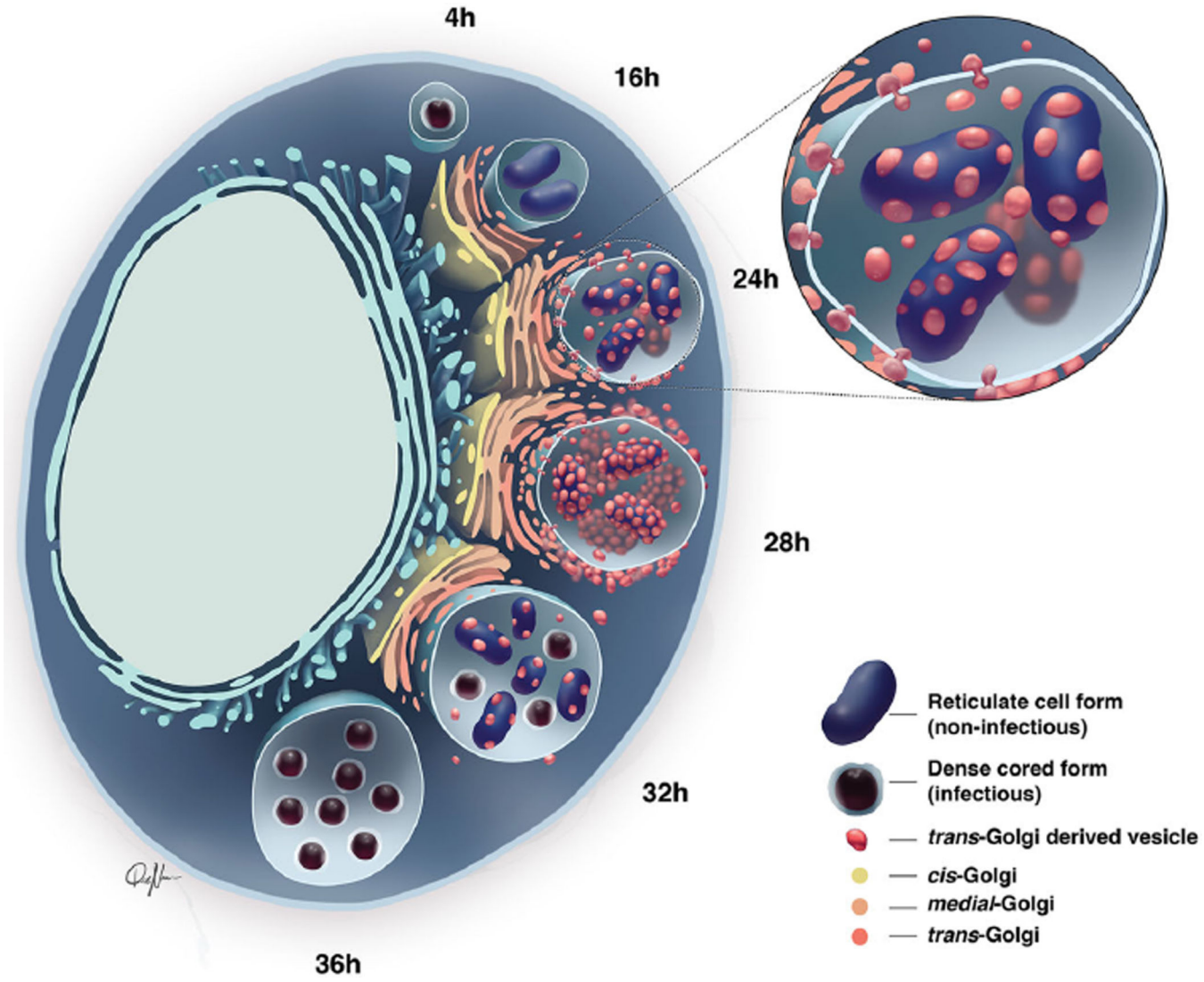

Fig. 12.

Model: Rab10-positive TGN vesicles are delivered into the ApV lumen and their association with replicative *A. phagocytophilum* RC organisms is a precursor for the bacteria to develop into the infectious DC form to complete the infection cycle. Between 12 and 16 h post-infection, after *A. phagocytophilum* has converted from the DC to RC form, the ApV has positioned itself in close proximity to the Golgi apparatus. By 24 h, the ApV has begun to intercept TGN-derived vesicles, which cross the AVM into the ApV lumen and associate with intravacuolar *A. phagocytophilum* RC organisms. TGN vesicle delivery into the ApV lumen and *A. phagocytophilum* association with TGN vesicles occurs around 28 h. Between 28 and 32 h, Rab10-positive TGN vesicle delivery into the ApV and association with intralumenal bacteria has waned considerably. Coincident with this phenomenon, TGN vesicle-negative *A. phagocytophilum* organisms have transitioned from the RC to DC form.